JGR Atmospheres

RESEARCH ARTICLE
10.1029/2023JD038645

Role of the Thermodynamic Structure of the Inner Core in Predicting the Intensification of Hurricane Patricia (2015)

Quanjia Zhong[1,2], Xu Lu[2], Xuguang Wang[2], Ruiqiang Ding[3], Wansuo Duan[1], and Zhaolu Hou[4]

[1]State Key Laboratory of Numerical Modeling for Atmospheric Sciences and Geophysical Fluid Dynamics (LASG), Institute of Atmospheric Physics, Chinese Academy of Sciences, Beijing, China, [2]School of Meteorology, University of Oklahoma, Norman, OK, USA, [3]Key Laboratory of Environmental Change and Natural Disasters of Chinese Ministry of Education, Beijing Normal University, Beijing, China, [4]Key Laboratory of Physical Oceanography/College of Oceanic and Atmospheric Sciences, Ocean University of China, Qingdao, China

Abstract We use short-range ensemble forecasts and ensemble clustering analysis to study the factors affecting the intensification of Hurricane Patricia (2015). Convection-permitting ensemble forecasts are classified into two groups: 10 spin-down (SPD) members and 10 spin-up (SPU) members with intensification rates of <0 and >0 m s^{-1} for the first 6 hr, respectively. Ensemble clustering analysis found that the wind–pressure relationship was incorrect in the SPD group, indicating that the SPD issue may be partly caused by an imbalance in the initial minimum sea-level pressure (MSLP) and the maximum wind speed (MWS). The SPD issue appears to be related to three main points: (a) a weaker upper-level warm core; (b) a drier inner core at low levels; and (c) a dry, cold air intrusion at mid-levels. In contrast, the SPU group has a stronger upper-level warm core and a relatively wet inner core at lower levels, as well as a relatively strong secondary circulation. These favorable initial conditions in the SPU group, combined with a greater updraft and stronger convection around the eyewall, result in more latent heating around or in the eyewall that favors the intensification of the tropical cyclone. Comparisons between the SPD and SPU groups suggest that the analyzed ensemble could not accurately capture the relationship between the initial MSLP and MWS, which, combined with the unfavorable thermodynamic conditions at the initial time, resulted in the incorrect evolution of the intensity. Therefore, improving the initial conditions appears to be an effective way to address the SPD issue.

Plain Language Summary Intensity spin-down (SPD) has been identified as a major issue in numerical hurricane models because maximum wind speed can decrease significantly and artificially in the first few hours of a simulation, thereby degrading the remainder of the intensity forecast. Ensemble clustering analysis was performed to explore the role of the thermodynamic structure of the inner core in predicting the intensification of Hurricane Patricia (2015). Convection-permitting ensemble forecasts are classified into SPD and spin-up (SPU) groups based on the intensification rates for the first 6 hr. Several statistically significant differences between the SPD and SPU members were found in the wind–pressure relationship, the upper-level warm core, moisture in the inner core, and secondary circulation. Particularly, the SPD issue may be partly caused by an imbalance in the initial wind–pressure relationship. Moreover, it also appears to be related to three main points: a weaker upper-level warm core; a drier inner core at low levels; and a dry, cold air intrusion at mid-levels. However, the intensification of the hurricane was sensitive to the upper-level warm core, moisture in the inner core, and secondary circulation. Overall, thermodynamic structure of the inner core plays a key role in predicting the intensification of Hurricane Patricia (2015).

Key Points:

- The spin-down issue may be partly caused by an imbalance in the initial wind–pressure relationship
- Intensification of the hurricane was sensitive to the upper-level warm core, moisture in the inner core, and secondary circulation
- The thermodynamic structure of the inner core plays a key role in predicting the intensification of Hurricane Patricia (2015)

Correspondence to:
X. Wang and R. Ding,
xuguang.wang@ou.edu;
drq@bnu.edu.cn

Citation:
Zhong, Q., Lu, X., Wang, X., Ding, R., Duan, W., & Hou, Z. (2023). Role of the thermodynamic structure of the inner core in predicting the intensification of Hurricane Patricia (2015). *Journal of Geophysical Research: Atmospheres*, *128*, e2023JD038645. https://doi.org/10.1029/2023JD038645

Received 10 FEB 2023
Accepted 17 JUL 2023

Author Contributions:
Funding acquisition: Xuguang Wang
Supervision: Xuguang Wang, Ruiqiang Ding
Visualization: Quanjia Zhong
Writing – original draft: Quanjia Zhong
Writing – review & editing: Quanjia Zhong, Xu Lu, Ruiqiang Ding, Wansuo Duan, Zhaolu Hou

1. Introduction

Accurate forecasts of tropical cyclones (TCs) intensity, especially in the rapid intensification phase, are a top priority for operational forecast centers. Efforts have been dedicated to improving the forecast skill of TC intensity by developing numerical models (Goldenberg et al., 2015), modifying the model physics (Chandrasekar & Balaji, 2016; Qin & Zhang, 2018), exploring various ensemble forecast methods (Lang et al., 2012; Sun et al., 2021), and assimilating novel observations into models through advanced data assimilation methods (Feng et al., 2022; Feng & Wang, 2019; Lu & Wang, 2021). However, large errors remain in intensity forecasts as a result of the lack of high-resolution observations and the limited ability of models with a coarse resolution to resolve the intensity, size, and structure of the TC (Feng & Wang, 2021; Lu, Wang, Tong, & Tallapragada, 2017;

B. Zhang et al., 2016). Previous studies have emphasized that an accurate representation of the inner core structure is essential for forecasts of TC intensity (Emanuel & Zhang, 2016; Emanuel et al., 2018).

Given the lack of adequate observations to depict the inner core structure, bogus vortex techniques are often used in early operational forecast systems to initialize the TC vortex based on the limited information available on the maximum wind speed (MWS), the radius of maximum wind (RMW), the minimum mean sea-level pressure (minimum sea-level pressure, MSLP), and the position of the TC center (Liu et al., 2006, 2020; Thu & Krishnamurti, 1992). With rapid advances in data assimilation techniques and better observing systems, the operational Hurricane Weather Research and Forecasting (HWRF) system is often used in combination with a vortex initialization scheme and a data assimilation system to generate the initial analysis for the TC intensity forecast (Tallapragada et al., 2014). In operational real-time forecasts of TCs, the vortex initialization scheme includes two components: vortex relocation to correct the position of the center of the TC and vortex modification to modify its intensity and size (Liu et al., 2020). After performing the vortex initialization, a variety of conventional, radar, and satellite data are assimilated into operational hurricane prediction models.

Many studies have reported that the accuracy of the intensity forecast may be enhanced by vortex initialization and data assimilation in the operational system (Lu, Wang, Li, et al., 2017; Pu et al., 2016; F. Zhang et al., 2011). However, intensity spin-down (SPD) has been identified as a major issue in numerical hurricane models because MWS can decrease significantly and artificially in the first few hours of a simulation, thereby degrading the remainder of the intensity forecast (Gopalakrishnan et al., 2018; Z. Zhang et al., 2020). Although this issue has been known for some time, intensity SPD remains challenging and is significant in some cases, especially in the prediction of intense TCs (Tallapragada et al., 2014; Zhou et al., 2015).

Efforts have been made to eliminate or at least reduce SPD over the last 10 years. Several modeling studies have suggested that the SPD issue may be attributed to a number of factors including: (a) deficiencies in the data assimilation algorithm; (b) unrealistic initial conditions as a result of the lack of observations of the inner core; (c) the complex interactions involved between the vortex initialization and data assimilation; (d) deficiencies in the model physics; and (e) the coarse resolution of the model (Bernardet et al., 2015; Lu & Wang, 2019; Pu et al., 2016; Zhou et al., 2015).

However, the above modeling studies normally used a single deterministic forecast to investigate the SPD issue, where they commonly proposed a scientific hypothesis that is related to the possible reason for the SPD issue occurrence, and then performed several sets of sensitivity experiments to confirm the hypothesis (Lu & Wang, 2019; Pu et al., 2016; Zhou et al., 2015). Such a deterministic approach has provided a better understanding of the SPD problem, but the conclusions may be case-dependent or limited by the sample size. For example, a case study of Hurricane Patricia (2015) by Lu and Wang (2019) reported that SPD can be mitigated in the deterministic forecast (control member) by modifying the vertical turbulence mixing and horizontal diffusion in the planetary boundary layer (PBL) scheme and an increase in both the horizontal and vertical resolution. Nevertheless, as discussed in the present paper, the vortex SPD problem is still notable in some members of an ensemble forecast, even if we use the same modified model configurations (e.g., horizontal, and vertical resolution) and physics parameterizations (e.g., PBL scheme) as the single deterministic forecast (control member). Other factors appear to be crucial to the intensity SPD of some members of the ensemble. It is therefore the scientific goal of this study to understand what crucial differences would lead to notable intensity SPD from an ensemble aspect.

Our previous study demonstrated that the low wavenumber structure of the initial wind analyses is crucial in the SPU process of Hurricane Patricia, compared with the high wavenumber components (Zhong et al., 2022). However, previous studies have reported that the thermodynamic aspects in terms of the upper-level warm core and low-level wet core also play a significant role in determining the changes in intensity of a TC (Emanuel & Zhang, 2017; Stern & Zhang, 2013; Tao & Zhang, 2014, 2019). For instance, D. L. Zhang and Chen (2012) demonstrated that the formation of an upper tropospheric warm core can contribute to the occurrence of rapid intensification. Emanuel and Zhang (2016) suggested that the uncertainties in forecasts of rapid intensity change are dominated by inner-core moisture errors in the initial conditions out to a few days. Therefore, a comparison was made of the initial temperature and moisture fields of the TC in this study. First, we will focus on the crucial differences in the initial thermodynamic structure of the TC between the SPD and SPU members. Second, we aim to investigate why the initial thermodynamic conditions in some ensemble members lead to vortex SPD and substantial degradation of the TC intensity forecast, but not those in other members.

Table 1
Model Configuration and Physical Parameterizations

	Model configuration used to produce the analysis ensemble	Model configuration used to perform the ensemble forecast
Model resolution	18/6/2 km	9/3/1 km
Vertical σ-level	61 levels (model top set to 2 hPa)	
Grid size	Outermost (288 × 576 grid points), intermediate (304 × 604 grid points), innermost (265 × 472 grid points)	Outermost (288 × 576 grid points), intermediate (304 × 604 grid points), innermost (303 × 604 grid points)
Planetary boundary layer (PBL)	HWRF PBL scheme (Hong & Pan, 1996)	HWRF PBL scheme (reduced horizontal diffusion weight from 0.75/3.0/4.0 to 0.75/1.0/1.2; modified turbulent mixing parameterization [vertical diffusivity profile modification])
Surface layer	HWRF modified surface layer scheme (Kwon et al., 2010)	
Land surface model	Noah land surface model (Ek et al., 2003)	
Microphysics scheme	Ferrier–Aligo microphysics scheme (Schoenberg Ferrier, 1994)	
Cumulus	Simplified Arakawa–Schubert cumulus scheme (Han & Pan, 2006)	
Radiation	RRTMG longwave and shortwave radiation schemes (Lacis & Hansen, 1974; Schwarzkopf & Fels, 1991)	

This paper is organized as follows. Overviews of Hurricane Patricia (2015), the model configuration, the ensemble experiment setup, and the analysis techniques are given in Section 2. In Section 3, for one set of retrospective ensemble forecasts, the SPD and SPU members are selected based on the rate of intensity change in the first few hours. Then, the key differences in the initial thermodynamic structure of the inner core between the SPD and SPU members are identified and their evolution with lead time is presented. Finally, Section 4 summarizes and discusses these results to address why the initial thermodynamic conditions lead to SPD only in some ensemble members.

2. Data and Methodology

2.1. Overview of Hurricane Patricia (2015)

Because of the notable SPD issue observed in HWRF, the intensification phase of Hurricane Patricia (2015) is used as a case study (Kimberlain et al., 2015). Hurricane Patricia (2015) developed in the eastern North Pacific at 0600 UTC on 20 October 2015. Rapid intensification began on 22 October 2015 and continued through 23 October 2015, reaching maximum intensity in terms of a MSLP of 872 hPa and a MWS of 95 m s^{-1} (Martinez et al., 2019). The hurricane then rapidly weakened and eventually made landfall in Mexico. Rogers et al. (2017) reported that the intensity of Patricia had an unprecedented rate of change of 54 m s^{-1} in a 24 hr period, much greater than the rapid intensification threshold of 15.4 m s^{-1} (Kaplan & DeMaria, 2003). None of the operational statistical and dynamical models were able to predict the rapid intensity change and peak intensity of Patricia during the rapid intensification stage. Here, we focus on the initial stage of rapid intensification at 1200 UTC on 22 October 2015 as MWS during Patricia intensified from 46.2 to 77.1 m s^{-1}.

2.2. Model Configuration and Experiment Setup

We used the gridpoint statistical interpolation (GSI)-based, continuously cycled, dual-resolution hybrid ensemble-variational (EnVar) data assimilation system for the operational HWRF model introduced by Lu, Wang, Tong, and Tallapragada (2017) to produce the ensemble analyses. During the data assimilation process, the vertical velocity and hydrometeors are initialized to zero in the model. Observations only affect the prognostic variables, such as surface pressure, wind, virtual temperature, and relative humidity. As a result, the analysis ensemble consists of 40 members plus a control member that only differs in the initial analyses of these prognostic variables. When generating the initial conditions, we used the same model configurations as those used in the 2015 operational HWRF model with horizontal resolutions of 18/6/2 km in the outer/middle/inner domains and 61 vertical levels (B. Zhang et al., 2016). The model top was set at 2 hPa. The model physics used in the data assimilation cycling were the same as those in the operational HWRF model (see Table 1). More details of the parameterization schemes and a description of the data assimilation system have been given by Lu, Wang, Tong, and Tallapragada (2017) and Tallapragada et al. (2014), respectively.

Owing to the small inner-core size of Patricia, the horizontal resolution of the model was increased to 9/3/1 km with a reduced domain size during the ensemble forecast. Correspondingly, the analysis ensemble was interpolated from the coarser 18/6/2 km to the finer resolution of 9/3/1 km before the ensemble forecasts. Specifically, the 9/3/1 km nests were aligned with the 18/6/2 km nests to improve the accuracy of the interpolation. The boundary conditions for the model were taken from the Global Forecast System forecast (GFS). The model physics used in the ensemble experiment followed those in the 2015 operational HWRF model (see Table 1), except that the vertical and horizontal diffusivities in the PBL parameterization were modified as described by Lu and Wang (2019).

In this study, one set of retrospective forecasts starting at 1200 UTC on 22 October 2015 was performed in the initial stages of rapid intensification of Hurricane Patricia (2015), and the experiments were output at hourly intervals for 12 hr. The use of higher frequency 1-hr

outputs rather than the standard 6-hr frequency helped us to better explore the effect of the initial conditions on the intensity change of the TC within the first few hours of the forecast. The best-track data for Hurricane Patricia (2015) were provided by the International Best Track Archive for Climate Stewardship (IBTrACS) project (Knapp et al., 2018). Specifically, the temporal resolution of the best track is officially 6 hr, and it was linearly interpolated to a 3-hr interval for more convenient comparison with the model output.

2.3. Ensemble Clustering Analysis Method

For the ensemble forecast with tens of members, one novel and effective method for identifying the key factors that lead to the SPD issues uses ensemble clustering analysis. In this study, ensemble clustering analysis is the task of grouping a subset of the members of an analyzed ensemble in such a way that members in the same group (a cluster) are more similar (in some sense) to each other than to those in other groups (clusters) (Johnson et al., 2011; Serafin et al., 2019; Yussouf et al., 2004; Weidle et al., 2013). There are several advantages of cluster analysis. Compared with random member selection, cluster analysis provides groups with structural similarity of features in a variable space. Accordingly, for one set of retrospective ensemble forecasts, we can focus our concern on the crucial differences in the initial analysis fields of the TC between a group of members with SPD and a group with spin-up (SPU, as depicted by the increase in the MWS). A second advantage of this method is that the difference in the intensity evolution of each cluster is seen clearly within the first few hours of the forecasts. Then, the possible mechanism for the TC intensification and the reasons behind the occurrence of SPD may be investigated using the ensemble clustering analysis.

As introduced in Section 2.2, the analysis ensemble members obtained from the data assimilation system only differ in their initial fields. To explore what crucial differences in the initial conditions lead to the different intensity evolution, ensemble members are first classified into SPD and SPU members (groups), which correspond to a rate of change of the TC MWS of <0 m s^{-1} for SPD and >0 m s^{-1} for SPU over the first 6 hr of the forecast. Based on these criteria, the SPD and SPU groups contain 10 and 30 members, respectively, with similar intensity evolution within each group. It was found that the intensification rates do not have a large spread among the 30 SPU members. Following our previous work (Zhong et al., 2022), we randomly selected 10 of the 30 SPU members to give equal numbers in each group and so create a homogenous sample.

3. Results

3.1. Temporal Evolution of the TC Intensity and the Wind–Pressure Relationship

Figure 1 shows the hourly outputs of the TC MSLP and MWS during the first 12 hr for the SPD and SPU groups. The SPD and SPU members both show an inconsistent variation between the MSLP and MWS during the first 3 hr, but this inconsistency is more significant in the SPD members than in the SPU members. The ensemble mean for the SPD group shows a significant decrease of about 9 m s^{-1} in the MWS and has a relatively steady MSLP during the first 3 hr (Figures 1a and 1c), whereas the SPU group shows an intensifying storm with an obvious decrease in the MSLP, but no significant decrease in the MWS (Figures 1b and 1d). After the first 3 hr of the forecast, although the ensemble mean for the SPD group shows the intensification of Hurricane Patricia, it is significantly degraded in the TC intensity forecast compared with the control member. During the same period, the decrease in the ensemble-averaged MSLP in the SPU group is consistent with both the control member and the observed best track, and the increase in the MWS is roughly comparable to the control member but slightly weaker than the observed best track.

As mentioned above, the MSLP and MWS are important metrics for the assessment of TC intensity. The control member can capture the SPU process of the storm during the first few hours forecast and the relationship between the MSLP and MWS is adequately reproduced in the deterministic forecast. To further explore whether the simulation of the wind–pressure relationship is reproduced in the ensemble members, we further calculate the differences in the MSLP and MWS between the ensemble and control members for the SPD and SPU groups. Scatter diagrams with regression lines show the relationship between the MSLP and MWS every 3 hr for the SPD and SPU groups (Figure 2). Generally, the magnitude of slope for the regression lines in the SPU group is greater than 1 hPa per m s^{-1}, whereas it is less than 1 hPa per m s^{-1} in the SPD group. As shown in Figures 2a and 2b, there are significant differences in the distribution of the scatter plots. The dots in the SPU group are nearer to or on the diagonal lines, which means the lower (higher) the MSLP, the larger (smaller) the MWS for the SPU members with respect to the control member. However, the dots in the SPD group show large deviations from the regression line, especially in Figures 2c and 2e, indicating similar MSLP values are associated with different

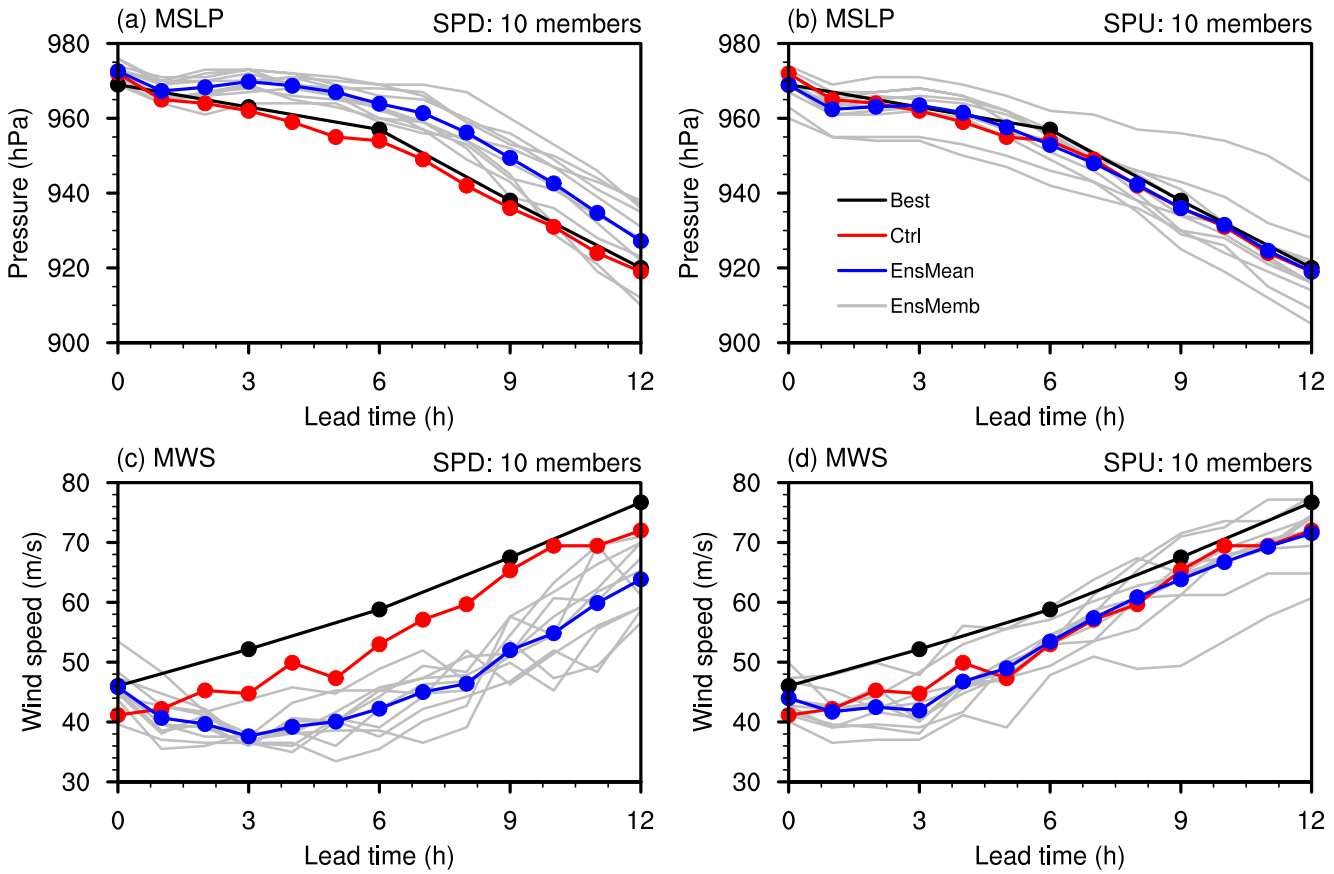

Figure 1. Forecasts of the minimum sea-level pressure (MSLP) and maximum surface wind speed (maximum wind speed, MWS) within the first 12 hr for the (a, c) spin-down (SPD) and (b, d) spin-up (SPU) groups. Gray lines represent ensemble members; blue lines denote the ensemble-average MSLP and MWS for the SPD and SPU groups; and red and black lines represent the control member and the best-track data, respectively.

MWS, and vice versa. Theoretically, as the TC intensity in the ensemble member is stronger (weaker) than that of the control member, the MSLP should be relatively lower (higher) and the MWS should be greater (smaller) in the ensemble member than those in the control member. The scatter plots essentially indicate that the relationship between the wind and pressure fields in the SPD groups is not as strong as that in the SPU groups at the initial time. Furthermore, some studies have suggested that the pressure-wind relationship is influenced by storm size, where larger TCs exhibit lower maximum sustained wind (MWS) compared to smaller TCs with the same MSLP (Chavas et al., 2017; Knaff & Zehr, 2007). In this study, the SPD group had a relatively large storm at the initial time with a mean RMW of approximately 47.29 km, while the SPU group represented a slightly smaller storm with a mean RMW of around 46.86 km. However, such a difference in storm size was not significant at the 95% confidence level and could not be one of the reasons for explaining the SPD issues.

Comparisons between the SPD and SPU groups indicate that the SPD issue in the ensemble forecasting of Hurricane Patricia is partly associated with an imbalance in the relationship between the initial MSLP and MWS. This imbalance results in significant model adjustment, leading to the occurrence of SPD issues. Recently, a case study of Hurricane Patricia (2015) by Tao et al. (2022) also suggested that a balanced TC circulation contributes to reducing the model adjustment time and giving a faster vortex SPU process in the simulation of the TC.

To check whether the structure of the initial vortex and its evolution are in dynamic balance at the boundary layer in the SPD and SPU groups, we analyzed the gradient wind balance relationship as described by the net radial force (NRF). Following previous work (Lu & Wang, 2019; Smith et al., 2009), we defined the NRF as the difference between the local radial pressure gradient force $-g\frac{\partial z}{\partial r}$ and the sum of the centrifugal force $\frac{v^2}{r}$ and Coriolis force $f_0 v$:

$$\mathrm{NRF} = -g\frac{\partial z}{\partial r} + \frac{v^2}{r} + f_0 v$$

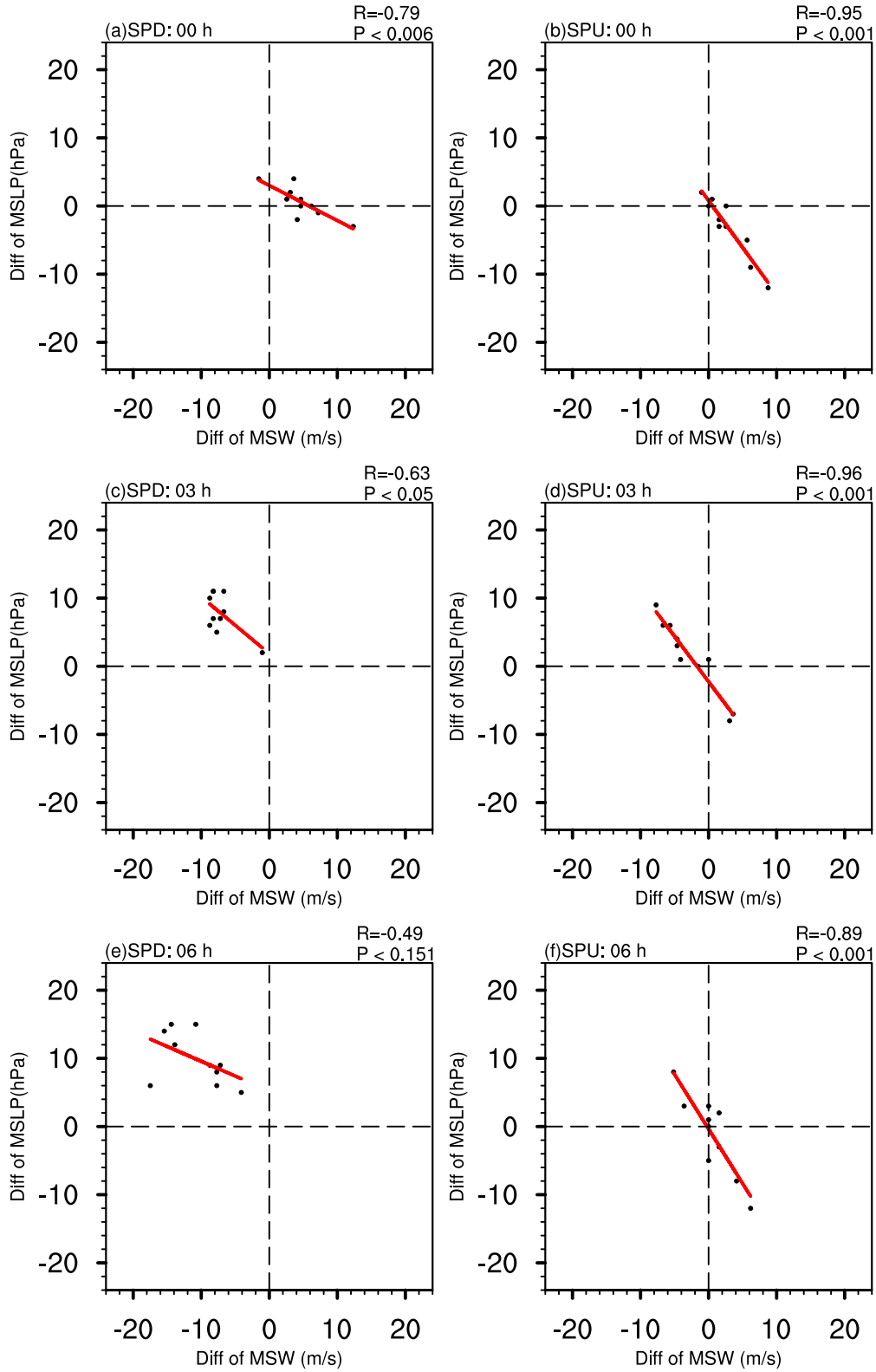

Figure 2. Scatter plots of the differences of the minimum sea-level pressure (MSLP) and maximum wind speed (MWS) between the ensemble and control members at every 3 hr forecast for the spin-down and spin-up groups. Dashed lines are the zero reference lines. Red lines denote the linear regression between the MSLP and the MWS. *R* and *P* indicate the correlation coefficient and its probability value, respectively. Note that the axes in each panel represent differences of each member from the control member at that particular lead time.

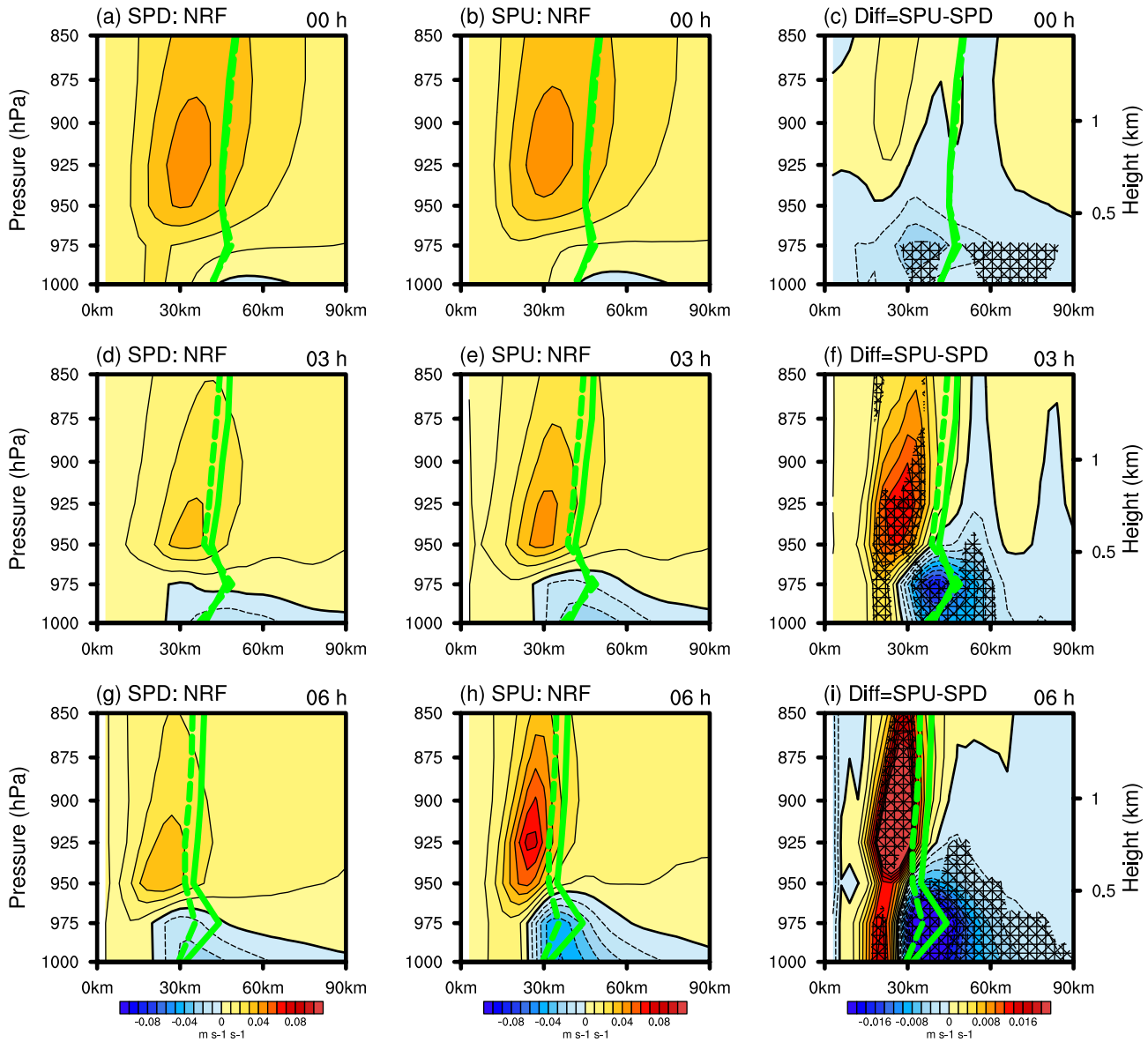

Figure 3. Radius–height plots of the azimuthal mean net radial force (NRF; m s^{-1} s^{-1}) below 850 hPa every 3 hr for the ensemble-average from (a, d, g) the spin-down (SPD) group and (b, e, h) the spin-up (SPU) group. (c, f, i) Differences in the ensemble-average NRF between the SPD and SPU groups (SPU minus SPD). Green dashed (solid) lines represent the average radius of maximum wind at each pressure level for the SPD (SPU) group. Hatched regions indicate statistical significance at the 95% confidence level.

where z is the geopotential height, v represents the azimuthal tangential wind, r represents the radial distance from the center of the storm, g is the gravitational constant, and f_0 is the Coriolis parameter. NRF = 0, NRF > 0, and NRF < 0 represent gradient wind balance, super-gradient flow, and sub-gradient flow, respectively.

The radius–height plots of the azimuthal mean NRF field below 850 hPa show that the two groups of ensemble members present similar distributions: a strong super-gradient flow in the inner core region throughout the boundary layer, but only a weak sub-gradient flow outside the RMW at 1,000 hPa (Figures 3a and 3b). This contrasts with the theoretical study of Smith et al. (2009), who indicated that a vertically varying structure with a super-gradient flow at the inner radii and a sub-gradient flow at the outer radii is found in the boundary layer of an intensifying storm. In a modeling study, Pu et al. (2016) suggested that the existence of strong super-gradient flow through the boundary layer is an indication of a dynamic imbalance at the inner radius, such that the model has had to adjust the wind–pressure relationship. In particular, the super-gradient flow (positive NRF) inside the

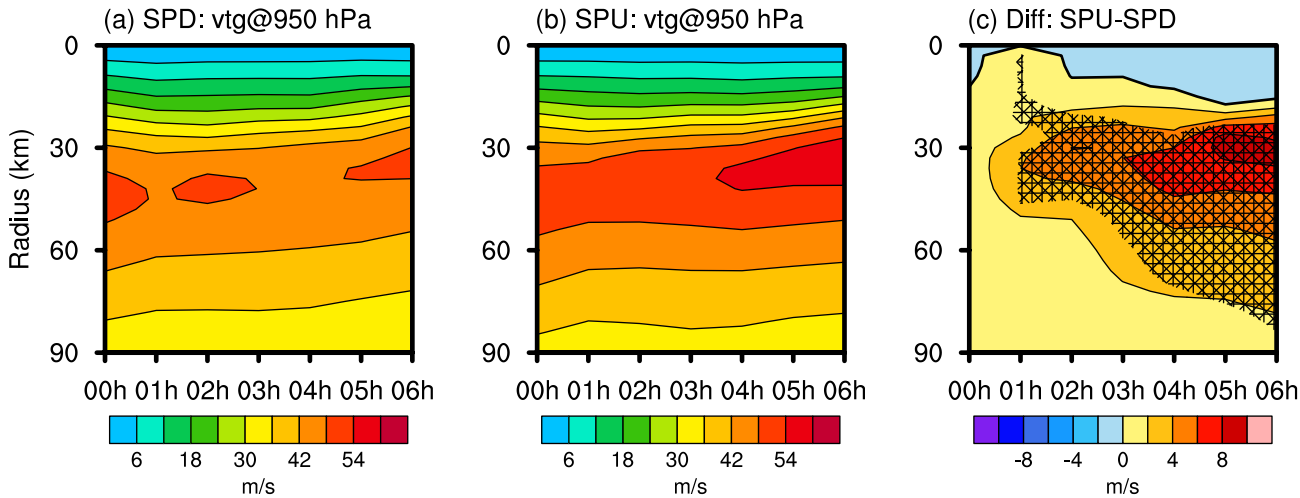

Figure 4. Time–radius Hovmöller plots of the ensemble-averaged azimuthal mean tangential wind (contours; m s^{-1}) at 950 hPa from the (a) spin-down (SPD) and (b) spin-up (SPU) groups. (c) Differences in the tangential wind between the SPD and SPU groups (SPU minus SPD). Hatched region represents statistical significance at the 95% confidence level.

RMW below 950 hPa in the SPU group is weaker than that in the SPD group (Figure 3c, significant at the 95% confidence level). Therefore, the model adjustment is slight and brief in the SPU group. Correspondingly, the MWS in the SPU members quickly recovers to the magnitude of the analysis and gradually increases afterward (Figures 1c and 1d). In contrast, the model adjustment is significant and prolonged in the SPD group, which leads to more persistent SPD.

After the first 3 hr of model adjustment, the SPD and SPU groups present a sub-gradient/super-gradient flow around the eyewall (Figures 3d and 3e). This is consistent with the theoretical study mentioned above (Smith et al., 2009). Specifically, the boundary layer inflows in the SPU group are more super-gradient in the inner core regions and more sub-gradient outside the inner core than those in the SPD group (Figure 3f), which is more favorable for the intensification of the TC (Smith et al., 2009). Therefore, the model takes less time to adjust these initial super-gradient imbalances for the SPU members than for the SPD members. At a lead time of 6 hr (Figures 3g–3i), similar features of a vertically varying NRF involving sub-gradient flow near the surface and super-gradient flow aloft are also seen, but the NRF distribution in the SPU group favors the intensification of TC more than that in the SPD group. Therefore, as clearly seen in Figures 1c and 1d, the 3–12-hr forecasts of the ensemble-averaged MWS in the SPD group are significantly weaker than those in the SPU group.

Because the change in the MWS is linked to the surface wind structure, we examine the evolution of the azimuthal mean tangential wind at 950 hPa (Figure 4). The initial vortex in both the SPD and SPU groups has a maximum of 44 m s^{-1} for the azimuthal tangential wind speed at around 45 km from the TC center. In the SPD group, there are three wind maxima at 00, 03, and 06 hr (Figure 4a). This temporal evolution is consistent with our primary conclusion: an initial vortex SPD in the MWS or a strong model adjustment of the wind speed field in the SPD group. For the SPU group, the tangential wind at a low level of 950 hPa steadily increases with time at and after a 3-hr lead time (Figure 4b). The initial tangential wind in the SPU group is slightly larger than that in the SPD group, but these differences are fairly small (Figure 4c). This is because the initial tangential winds among the SPU members are not consistently larger than those among the SPD members.

3.2. Differences in the Thermodynamic Properties of the SPD and SPU Groups

Other key factors, apart from the gradient wind imbalances, affecting the different evolutions of intensity in the SPD and SPU groups remain unknown. Many studies have shown that the evolution of an upper tropospheric warm core coincides with rapid TC intensification (Chen et al., 2015; Stern & Nolan, 2012; D. L. Zhang & Chen, 2012).

To understand how the warm core relates to different intensity forecasts of the hurricane in the SPD and SPU members, we further explore the evolution of the perturbation temperature with respect to the environmental

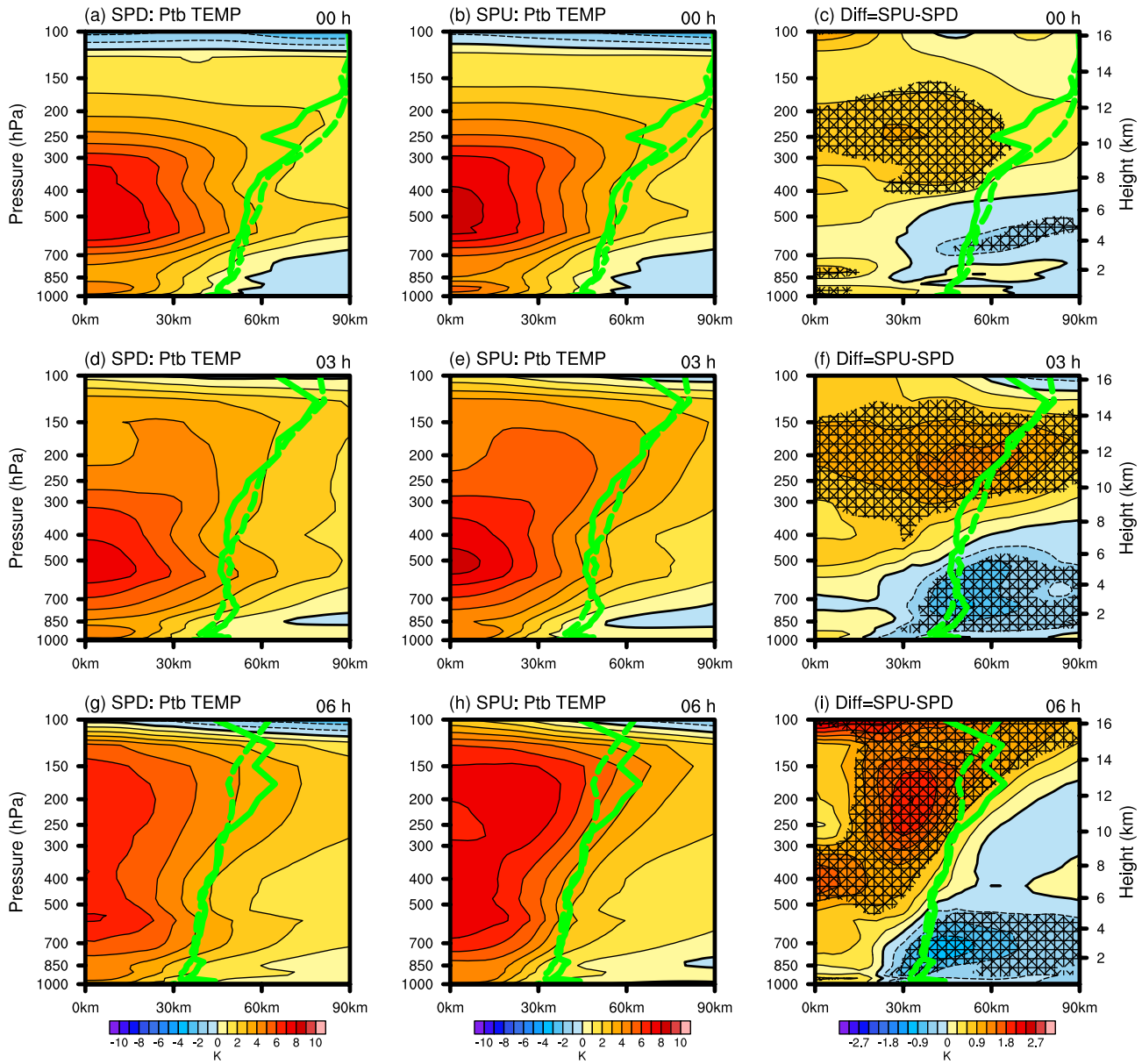

Figure 5. Radius–height plots of the ensemble-averaged azimuthal mean perturbation temperature (K) every 3 hr from the (a, d, g) spin-down (SPD) and (b, e, h) spin-up (SPU) groups. (c, f, i) Differences in the mean perturbation temperature between the SPD and SPU groups (SPU minus SPD). Green dashed (solid) lines represent the average radius of maximum wind at each pressure level for the SPD (SPU) group. Hatched regions indicate statistical significance at the 95% confidence level.

temperature and determine their differences between the two groups using the ensemble clustering analysis (Figure 5). Considering the small size of Hurricane Patricia, the perturbation temperature was calculated as the difference between the local temperature in the inner core region and the environmental temperature averaged in an annulus with radius of 300–500 km at each corresponding altitude. The warm core structure was characterized by its strength and the height of the maximum perturbation temperature.

Figures 5a and 5b clearly show that the ensemble-averaged warm core strength of about 8 K is found at 500 hPa at the initial time for the SPD group, slightly weaker than the 9-K warm core strength for the SPU group at the same level. The model system produces a relatively warmer inner core throughout the troposphere for the SPU group than for the SPD group, especially from 400 to 200 hPa. The SPU group is also relatively cool outside the inner core region below 500 hPa (Figure 5c). The results here confirm that a key factor in the maintenance and intensification of the TC is the relatively warm inner core at upper levels in the SPU group. This is consistent with

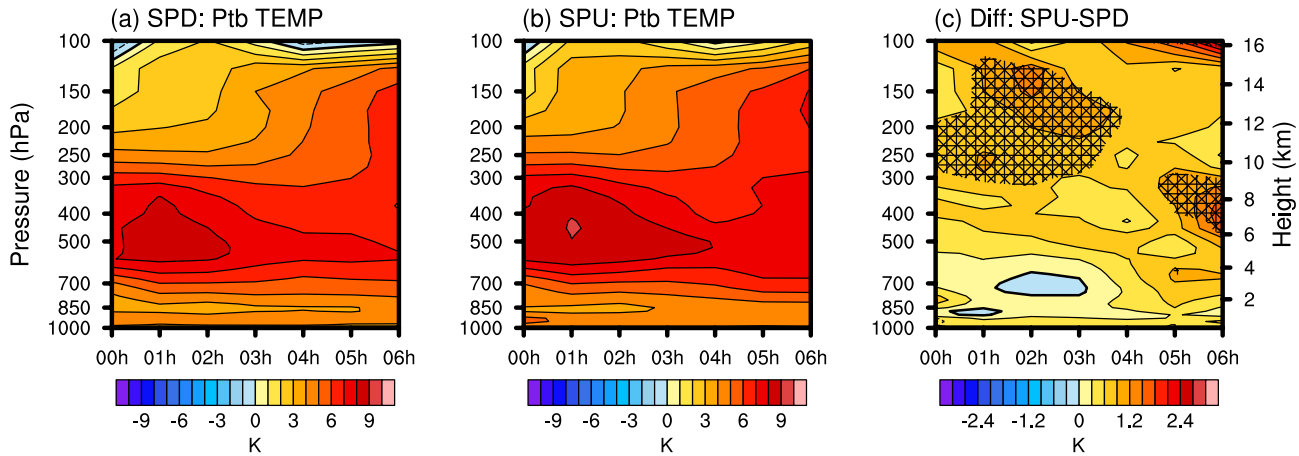

Figure 6. Time–radius Hovmöller plots of the ensemble-averaged perturbation temperature (contours; K) at tropical cyclone center for the (a) spin-down (SPD) and (b) spin-up (SPU) groups. (c) Differences in the perturbation temperature between the SPD and SPU groups (SPU minus SPD). Hatched region represents statistical significance at the 95% confidence level.

a previous study of Shi and Chen (2021) who indicated that the TC intensity generally increases with the strength of the warm core. In contrast, for the SPD group, combining the results from Figures 3c and 5c shows the weaker upper-level warm core that is unfavorable for the intensification of the TC and a relatively strong super-gradient imbalance, which leads to a significant intensity adjustment.

After 3 hr of the model forecast or adjustments, the warm core weakens in the SPD group, but the strength of the warm core in the SPU group does not change much during the same period (Figures 5d and 5e). There is a significant difference in the warm core between the SPD and SPU groups, which is positive at high levels above 300 hPa and negative outside the RMW at mid- and low levels below 500 hPa (Figure 5f). Correspondingly, the ensemble-averaged decrease in the MWS persists in the SPD group while the ensemble-averaged MWS in the SPU group is almost steady at about 42 m s^{-1} during the first 3 hr (Figures 1c and 1d). Over the 3–6-hr period of the forecast, the MWS is almost steady in most of the SPD members and the ensemble-averaged MWS is comparable to the magnitude of the initial ensemble mean MWS at a lead time of 6 hr as a result of the weakening of the warm core in the SPD members (Figure 5g). However, in the SPU group, rapid intensification occurs, after which rapid warming occurs in the perturbation temperature field (Figure 5h). This difference shows that the upper-level warm core in the SPU group is stronger, higher, and more persistent than that in the SPD group, resulting in the storm intensification (Figure 5i).

We further compare the temporal evolutions of the warm core between the two groups. In the SPD group, there is a warm core with a temperature anomaly of 8 K at the mid-level between 400 and 600 hPa, but this is only maintained within the first 2-hr forecast. Then, its strength generally weakens, while its height decreases with forecast time (Figure 6a). However, in the SPU group, the strength of the warm inner core decreases more slowly and the warm core maintains a nearly constant pressure height of 500 hPa until a lead time of 4 hr (Figure 6b). Within the first 3-hr forecast, the upper tropospheric perturbation temperature in the SPU group is larger than that in the SPD group (Figure 6b). The results shown in Figures 5 and 6 indicate that initial differences in the warm core are associated with the SPD issue and the accurate depiction of the warm core structures of TCs is of particular importance in predicting TC intensification. As emphasized by Yanai (1964), the thermal structure of the warm core has a significant role in driving the three-dimensional circulation and in TC kinetic energy budgets.

In addition to the temperature field, the amount of moisture in the inner core is another major factor affecting the intensity and structure of a TC (Emanuel & Zhang, 2017; F. Q. Zhang & Sippel, 2009). Figure 7 shows the averaged azimuthal specific humidity from the initial time to a lead time of 6 hr and the differences between the SPD and SPU groups. Following the definition of the perturbation temperature, the perturbation specific humidity was calculated relative to the mean environmental humidity derived from the 300–500-km radius annulus at each corresponding pressure level. In the initial condition, a maximum perturbation specific humidity is found inside the inner core region at a low level of about 850 hPa for the SPD and SPU groups (Figures 7a and 7b). Significant differences in the perturbation specific humidity between the SPD and SPU groups are clearly seen

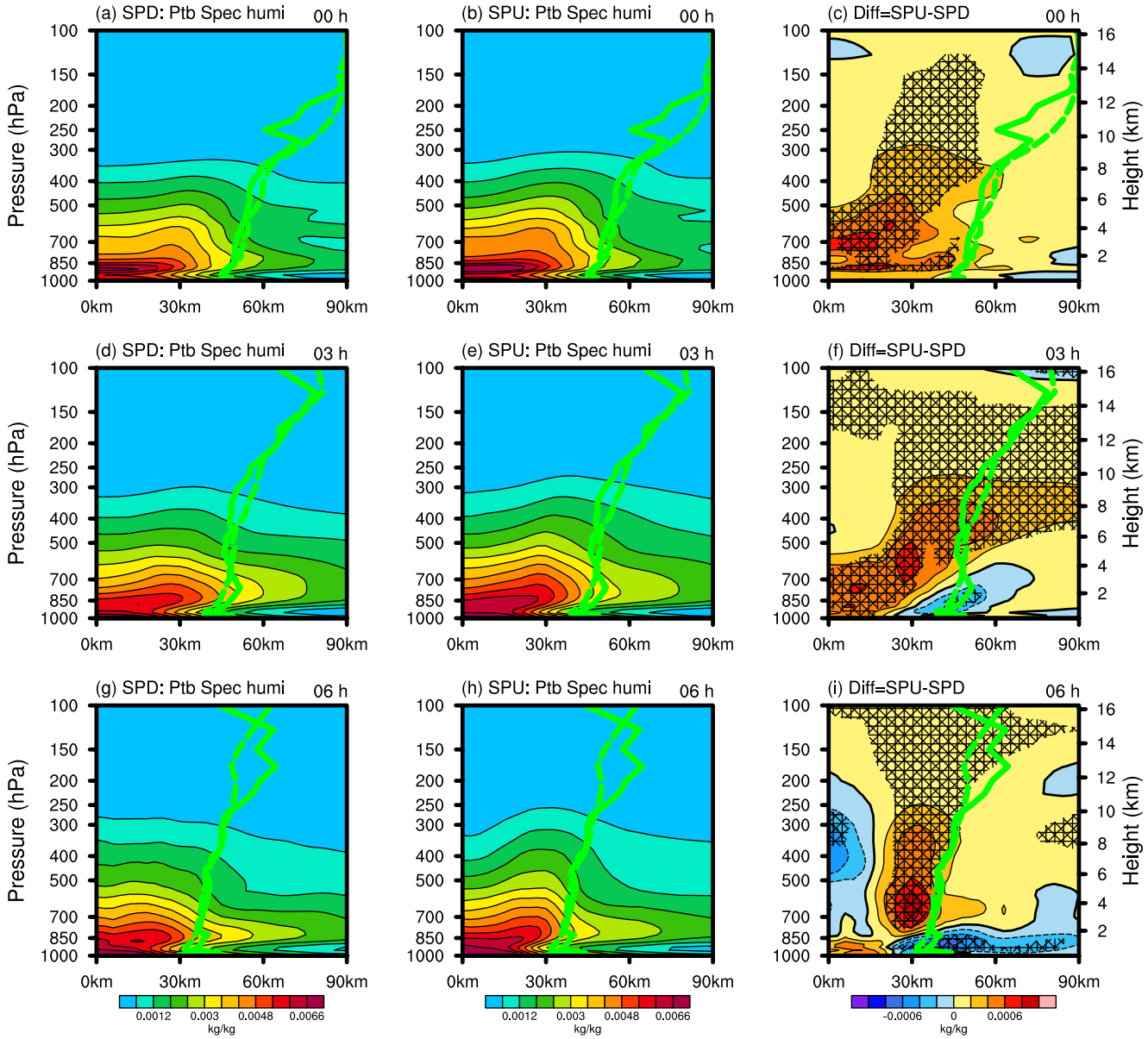

Figure 7. As in Figure 5, but for the azimuthal mean specific humidity (kg kg^{-1}).

inside the RMW, especially at mid- and low levels below 500 hPa (Figure 7c). Such differences can be considered as an important factor for the different intensity evolutions between the two groups. Theoretically, the SPU group presents a relatively wet inner core structure, providing more moisture to yield stronger convection. In contrast, the relatively dry inner core structure in the SPD group provides less moisture and thus inhibits convection. F. Q. Zhang and Sippel (2009) reported that the intensity change of a TC may be largely dependent on internal dynamics processes and moist convection. Van Sang et al. (2008) suggested that a relatively wet inner core, in combination with higher initial instability, may lead to a stronger mean upward velocity and generate more precipitation with a greater release of diabatic heat, which is unfavorable for the intensification of a TC.

Within a short period of the 3-hr forecast, the strength of the wet inner core structure slightly weakens in both groups (Figures 7d and 7e). There is a relatively wet inner core structure in the SPU group, except for the regions around the RMW below 700 hPa. Significant differences in perturbation specific humidity between the two groups are present both within and outside the inner core region over the first few hours (Figure 7f). After 6 hr of the model forecast, the SPU group is drier than the SPD group in the TC center at mid-levels and outside

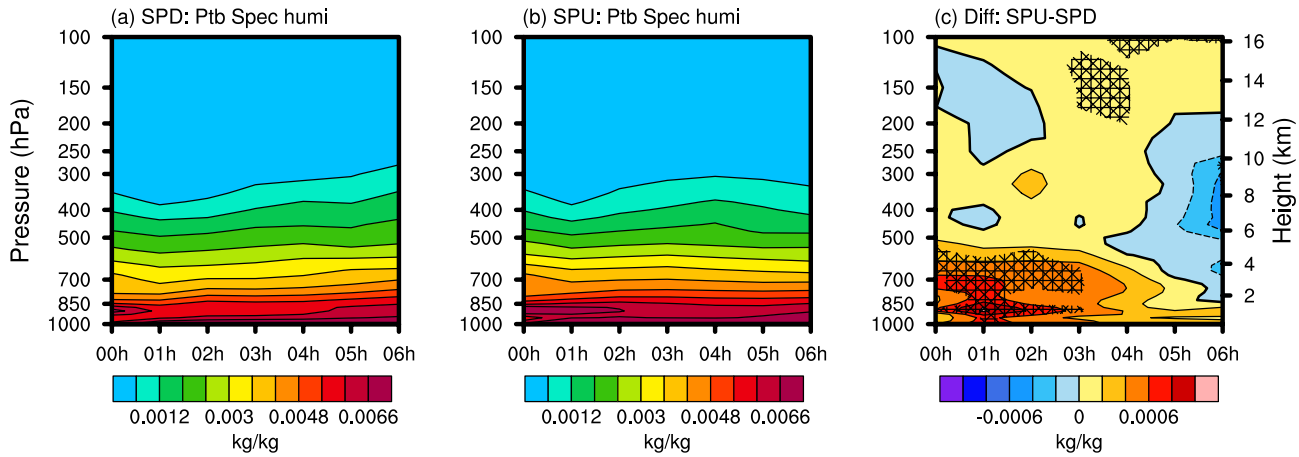

Figure 8. Time–radius Hovmöller plots of the ensemble-averaged perturbation specific humidity (contours; kg kg^{-1}) at tropical cyclone center for the (a) spin-down (SPD) and (b) spin-up (SPU) groups. (c) Differences in the perturbation specific humidity between the SPD and SPU groups (SPU minus SPD). Hatched region represents statistical significance at the 95% confidence level.

the RMW below 850 hPa, whereas it is wetter than the SPD group around the eyewall from 850 to 100 hPa (Figures 7g–7i). Figures 8a and 8b show a consistent decrease in perturbation specific humidity from boundary layer to tropopause in both groups. A comparison of the radius-height plots of the azimuthally averaged perturbation specific humidity at the TC center between the SPD and SPU groups also shows that there are significant differences in the inner core moisture below 500 hPa at the first 3-hr forecast when the SPD group is affected by the SPD issue. This is consistent with the results shown in Figure 7, where there is relatively high perturbation specific humidity in the inner core below 500 hPa during the first 3 hr in the SPU group but a relatively low perturbation specific humidity in the SPD group. Such differences in the wet core may cause different evolutions of the TC intensity.

To better distinguish intensity changes solely attributed to moisture, temperature differences, and their combined effects, we present a detailed analysis of the relative humidity evolutions in the SPD and SPU groups (Figure 9). The radius-height distribution of relative humidity exhibits significant differences between the two groups, following similar trends observed in the perturbation specific humidity plots. Notably, the presence of the eye is clearly evident in the relative humidity distribution, whereas it appears less pronounced in the specific humidity distribution. Furthermore, the relative humidity distribution indicates that neither group has fully developed a saturated eyewall, although the SPU group demonstrates greater proximity to achieving it. In contrast, the specific humidity distribution alone cannot definitively determine the presence of a saturated eyewall. These findings underscore that the SPD issues cannot be solely attributed to differences in moisture but also arise from initial disparities in the temperature field.

Figure 10 illustrates the temporal evolution of the vertical velocity of Hurricane Patricia (2015). Because the vertical velocity is reset to zero when it is initialized in the model, we use the vertical velocity at the 1-hr forecast to represent the initial vertical velocity. Both the SPD and SPU groups have two prominent maxima around a 30–60-km radius from the TC center, with a lower maximum at 850–700 hPa and an upper maximum at 250–150 hPa (Figures 10a and 10b). There are four regions of significant difference in the vertical velocity between the SPD and SPU groups (Figure 10c): the TC center at 500 and 200 hPa, around the 30-km radius at 500–300 hPa, and around the 90-km radius at 500–150 hPa. At the initial time, unlike the SPD group, the SPU group has two minima of vertical velocity in the TC center in the upper and lower troposphere, indicating that the SPU group has a weak downdraft in the TC center. D. L. Zhang and Chen (2012) showed that the onset of TC rapid intensification accomplishes the development of an upper tropospheric warm core associated with descending stratospheric air in the TC eye. Consistently, as shown in Figures 5a–5c, a stronger upper-level warm core appears in the SPU group. In addition, the SPU group also has larger vertical velocity around a 30–60-km radius than the SPD group, indicating that the convective updraft in the SPU group is stronger than that in the SPD group around the RMW. Therefore, moist convection can be effectively initiated by the stronger updraft in combination with a relatively wet core in the boundary layer shown in Figures 7a–7c.

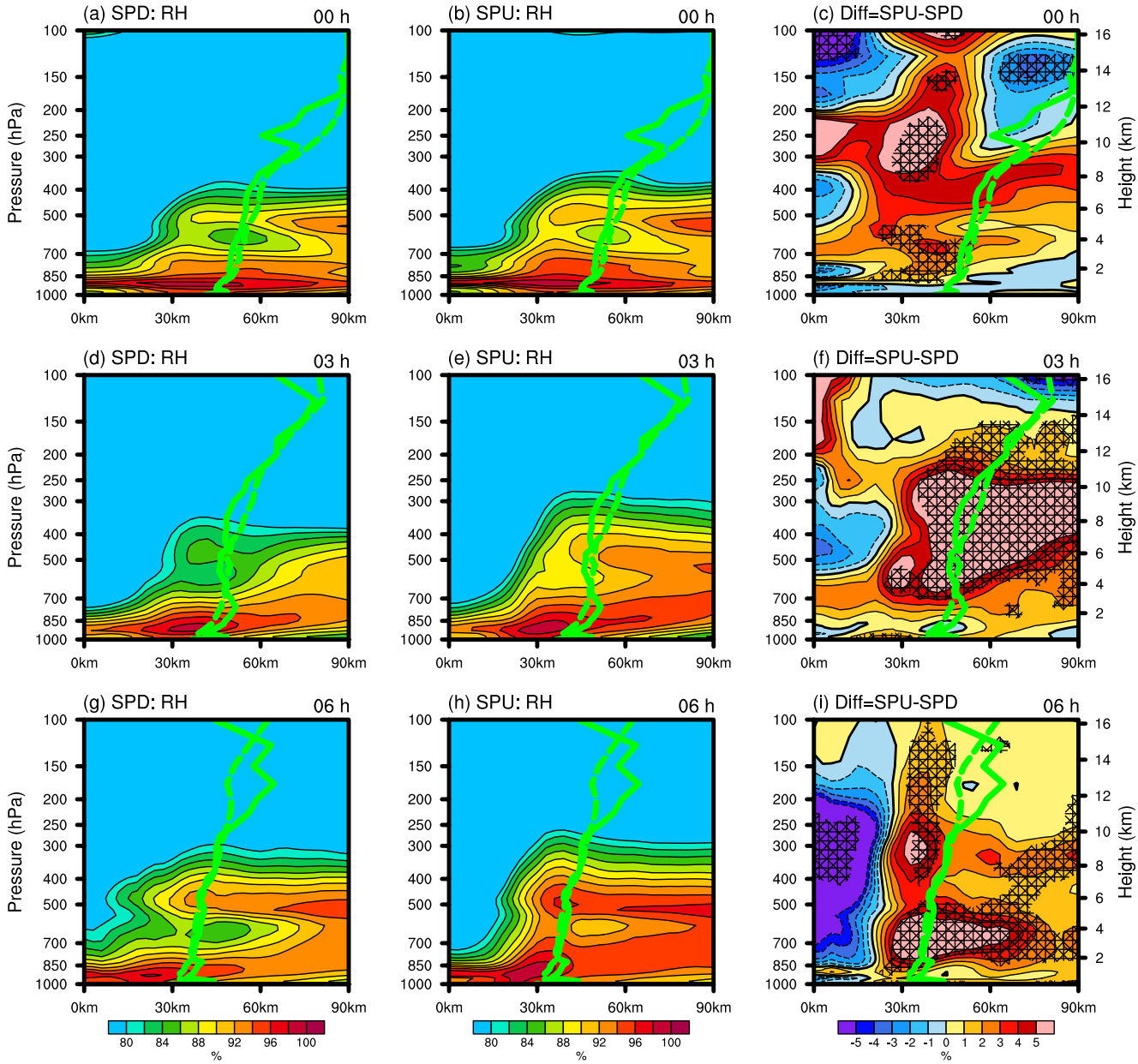

Figure 9. As in Figure 5, but for the azimuthal mean relative humidity (%).

After the 3-hr forecast, the two prominent centers of maximum vertical velocity evolve to a single maximum in the upper level (Figures 10d and 10e), indicating the development of convection and the subsequent formation of the eyewall. In the first 3-hr lead time, the difference in vertical velocity between the SPD and SPU groups (comparing Figures 10a and 10b with Figures 10d and 10e) is negative in the TC center and positive at about 30–60-km radius (Figures 10c and 10f). After the 6-hr forecast, there are two centers of maximum vertical velocity at about 200 hPa in the SPD group, but only one center with a significant lateral variation in the velocity in the SPU group (Figures 10g and 10h). The vertical velocity at 30-km radius in the SPU group is significantly larger than that in the SPD group (Figure 10i).

Although the above ensemble clustering analysis suggests significant differences in both magnitude and distribution of the vertical velocity at 1-hr lead times between the two groups (Figure 10c), it should be noted that such differences are not the primary causes of the SPD issue. This is because the lack of initial vertical velocity would add a stochastic element to intensity forecasts. Several studies have suggested that eyewall formation is the

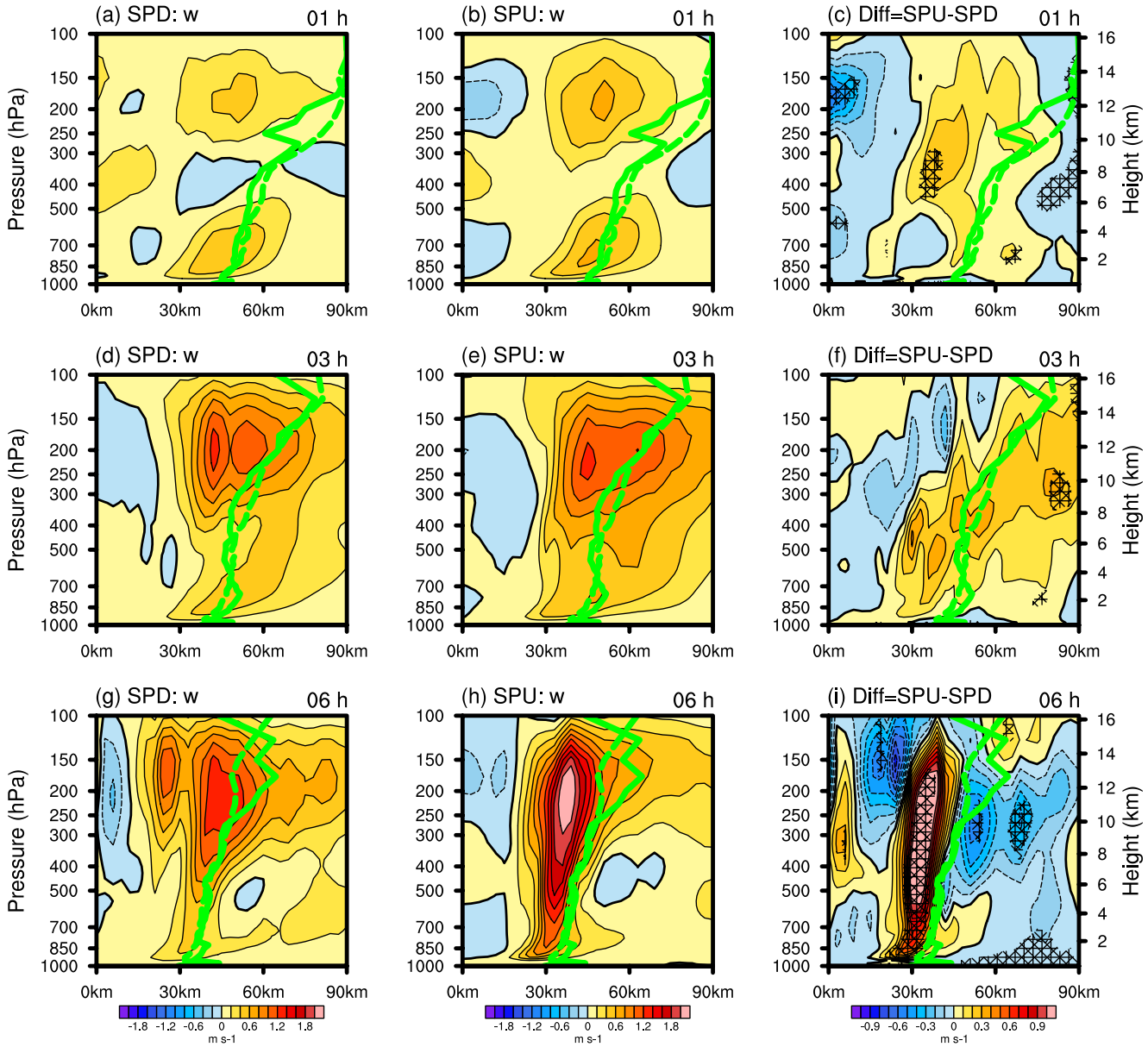

Figure 10. As in Figure 5, but for the azimuthal mean vertical velocity (m s^{-1}).

major mechanism for TC intensification (Heng & Wang, 2016; Pu et al., 2009). In an early study, Pu et al. (2009) revealed that a more realistic initial eyewall and vortex structure is necessary for a more accurate forecast of TC rapid intensification. Heng and Wang (2016) also suggested that diabatic heating associated with convection in the eyewall plays a critical role in the intensification and maintenance of a TC. As the vertical velocity is initially reset to zero, the subsequent difference in the vertical velocity at 1-hr lead time mainly results from the initial differences of other factors (e.g., dynamic and thermodynamic properties). As shown in Figures 10e and 10h, given the lack of vertical velocity at the initial time, it takes up to 6 hr for a realistic eyewall to even develop in the SPU group. This could obviously have huge implications for the intensity evolution given the absence of any initial vertical velocity or eyewall. This result agrees with the study of Vukicevic et al. (2013), who reported that one of the major reasons leading to the SPD problem is the resetting of the vertical velocity to 0 within the HWRF system.

Figure 11 illustrates the temporal evolution of the radius–height cross section of the radial wind and secondary circulation. The initial radial wind outside a 30-km radius shows a quadrupole-like structure in the vertical

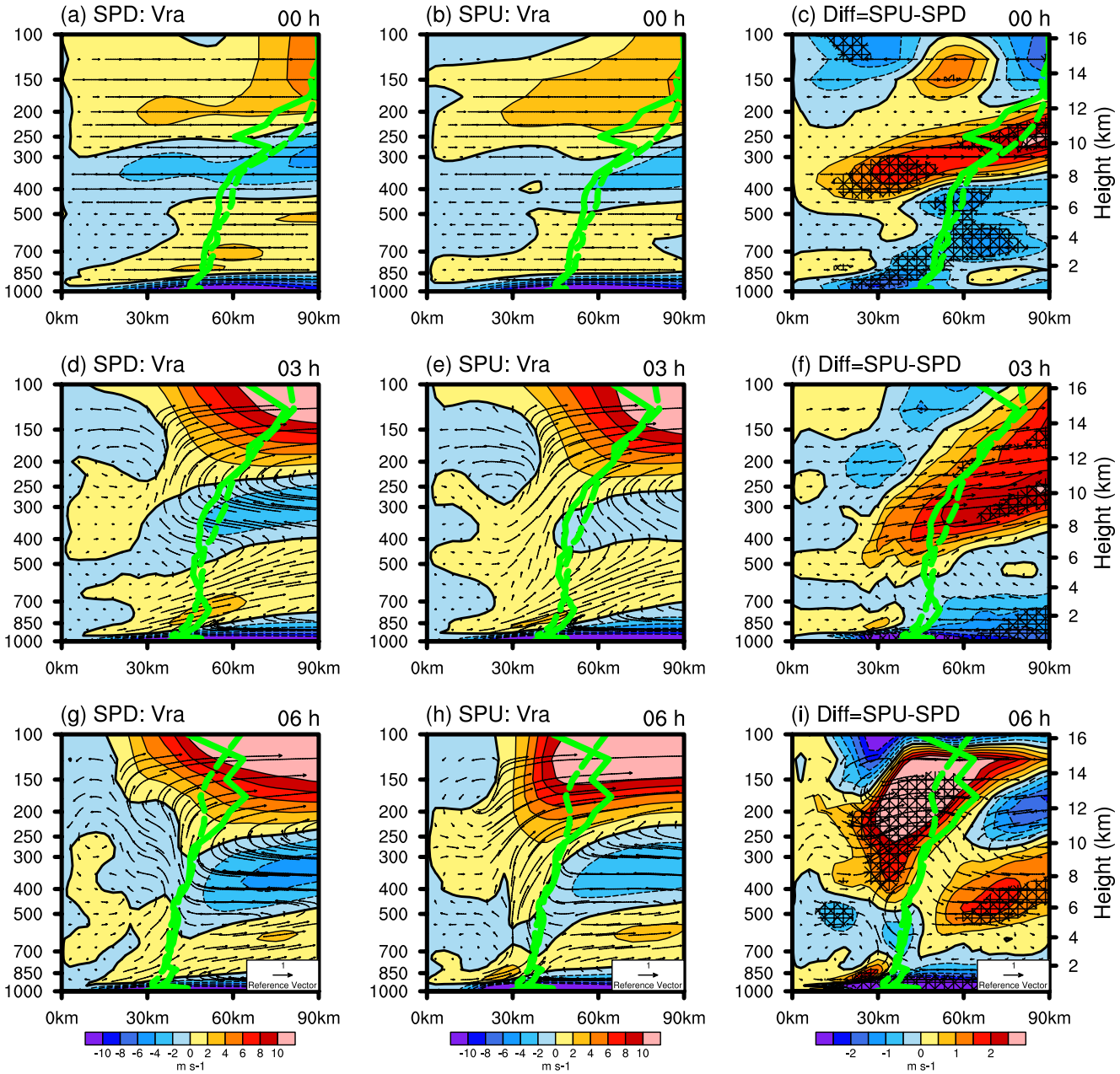

Figure 11. Radius–height plots of ensemble-averaged azimuthal mean radial wind (shading; m s^{-1}) and secondary circulation (vectors; m s^{-1}) every 3 hr for the (a, d, g) the spin-down (SPD) and (b, e, h) the spin-up (SPU) groups. (c, f, i) Differences in the mean radial wind and secondary circulation between the SPD and SPU groups (SPU minus SPD). Green dashed (solid) lines represent the average radius of maximum wind at each pressure level for the SPD (SPU) group. Hatched regions indicate statistical significance at the 95% confidence level.

direction in both the SPD and SPU groups, characterized by a negative radial wind at the boundary layer below 850 hPa, a positive radial wind at low levels between 500 and 850 hPa, a negative radial wind at mid-levels between 300 and 500 hPa, and a positive radial wind at upper levels above 300 hPa. This indicates that the initial secondary circulation involves several major components: a strong boundary layer inflow; a strong upper-level outflow; a strong eyewall updraft in association with the boundary layer inflow and upper-level outflow; a weak outflow in the mid- and low levels related to the overturning circulation; a weak inflow in the mid- and upper levels with the intrusion of dry cold air; and a weak eye downdraft (Figures 11a and 11b). Compared with the SPU group, the SPD group shows a weaker boundary layer inflow, but stronger overturning and a stronger intrusion of dry, cold air in the mid- and upper levels could contribute to the SPD problem (Figure 11c). Specifically,

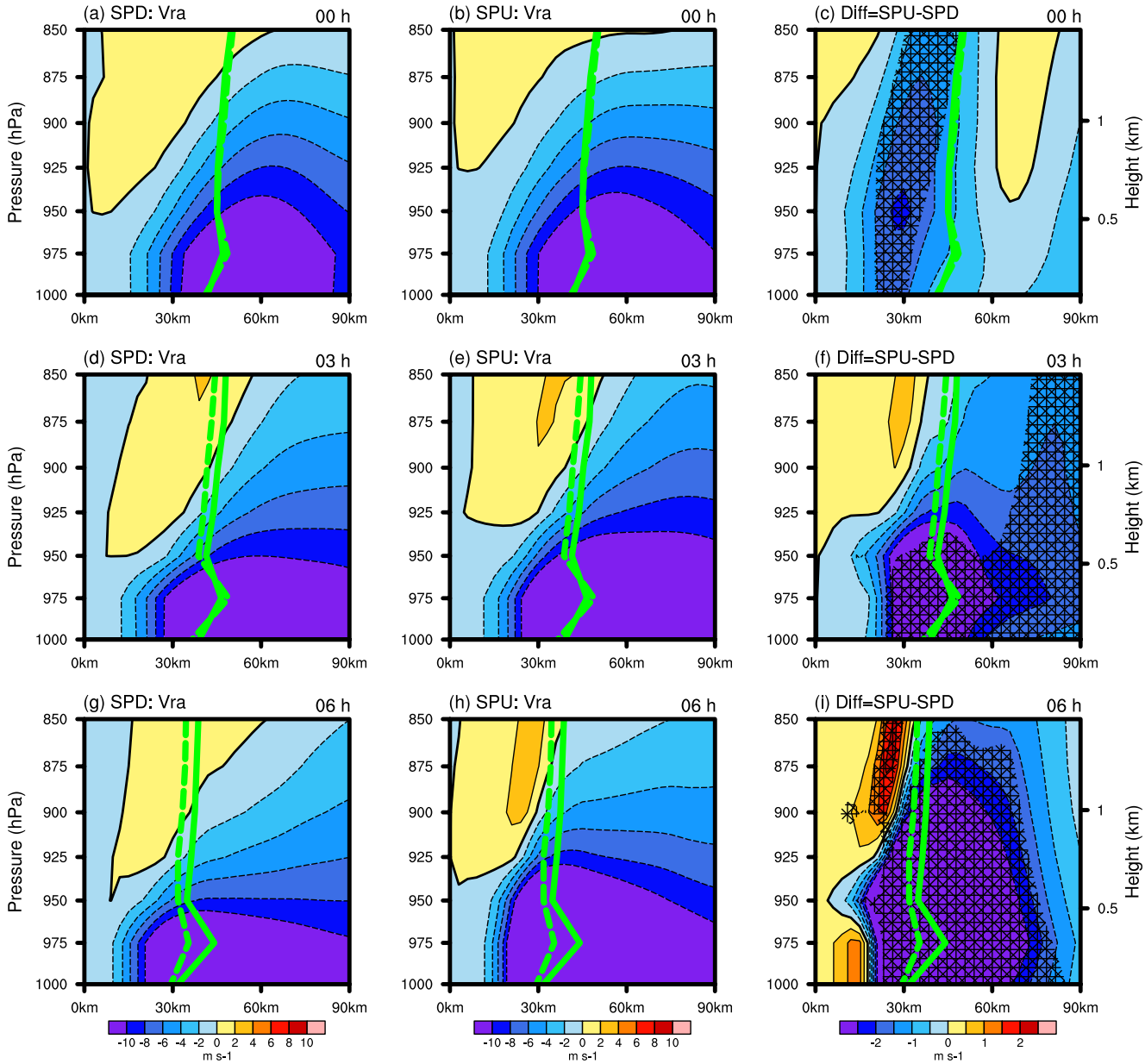

Figure 12. Radius–height plots of ensemble-averaged azimuthal mean radial wind (shading; m s^{-1}) below 850 hPa every 3 hr for the ensemble-average from (a, d, g) the spin-down (SPD) group and (b, e, h) the spin-up (SPU) group. (c, f, i) Differences in the ensemble-averaged mean radial wind between the SPD and SPU groups (SPU minus SPD). Green dashed (solid) lines represent the average radius of maximum wind at each pressure level for the SPD (SPU) group. Hatched regions indicate statistical significance at the 95% confidence level.

the inflow layer depth in the SPD group is smaller compared to that in the SPU group, and there are notable discrepancies in the radial winds, particularly around the 30-km radius at 1,000–850 hPa (Figures 12a–12c). Previous studies have suggested that relatively weak boundary layer inflow does not favor intensification of the TC (Guo & Tan, 2017), and dry air intrusion would weaken a TC by inducing asymmetric convective activity (Tao & Zhang, 2014; Wu et al., 2015).

A comparison between Figures 11d and 11g and Figures 11e and 11h shows that the inflow of dry cold air across the RMW region between 300 and 500 hPa in the SPD group is significantly stronger than the radial inflow in the SPU group, whereas the upper-level outflow above 300 hPa and outside a radius of 50 km is relatively weaker in the SPD group (Figures 11f and 11i). During the first 6 hr, the depth of the inflow layer decreases in the SPD group (Figures 12g and 12f), while it increases in the SPU group (Figures 12e and 12h). These variations in the

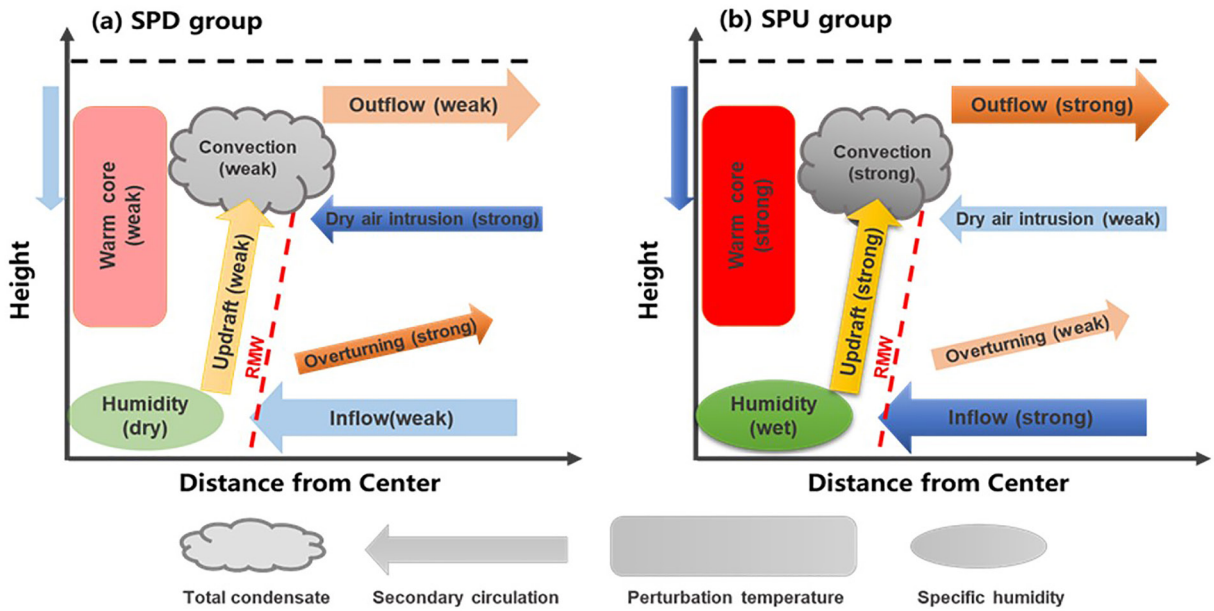

Figure 13. Schematic diagrams of the tropical cyclone structure in the spin-down and spin-up groups.

inflow layer depth may be related to the different evolutions of the TC intensity (Figures 12f and 12i). Overall, both in the structures with a weak upper warm core and a decrease in the radius of the region of warm perturbation temperature from 1,000 to 100 hPa and in the structures with a moist inner core with a low perturbation humidity at upper levels (Figures 5 and 7), the intrusion of dry, cold air induced by the stronger inflow in the SPD group breaks the secondary circulation and does not favor storm intensification.

4. Summary and Discussion

We have investigated the MWS SPD issues in the ensemble prediction of Hurricane Patricia (2015) through ensemble clustering analysis. The results show that the SPD issue may be partly caused by the imbalance in the initial MSLP and wind fields. Moreover, we carried out further analyses of the other causes of the different temporal evolution of the TC intensity in the SPD and SPU groups. Figure 13 is a schematic diagram showing the initial differences in the structure and intensity of Hurricane Patricia in these two groups.

In the initial conditions of the analysis ensemble, the SPD group has a stronger super-gradient imbalance inside the RMW below 950 hPa than the SPU group. As a result, the SPD group takes more time for the wind–pressure relationship to adjust in the model. In the SPD group, we see that a weak warm core in the upper troposphere, a relatively low specific humidity, and a weak inflow layer in the lower troposphere provide unfavorable initial conditions in the inner core for the intensification of the TC. During the first few hours, the decay of an upper tropospheric warm core associated with the weak stratospheric downdrafts in the TC eye coincides with the adjustment of the wind–pressure relationship in the model. It is well known that the convective updraft with the release of latent heat and energy conversion around the eyewall plays a critical role in the intensification and maintenance of a TC (Li & Pu, 2008; Zheng et al., 2020). However, the relatively weak updraft around the eyewall is related to the intrusion of dry air into the inner core as a result of the relatively strong inflow at mid-levels. At the same time, the relatively dry inner core structure resulting in less moisture supply combined with the relatively weak updraft inhibits convection. These processes lead to a significant intensity SPD within the first 3 hr and substantial degradation of the forecast of the intensity (Figure 13a).

In contrast, the SPU group exhibits several distinct characteristics relative to the SPD group at the initial time: (a) the inflow is more sub-gradient and the eyewall is more super-gradient; (b) the azimuthally-averaged tangential wind is stronger; (c) the warm core is warmer; (d) the inner core has more moisture; (e) the 1-hr vertical velocities are stronger in the eyewall and weaker in the eye; and (f) the secondary circulation is stronger, with stronger surface inflow and stronger outflow between 500 and 200 hPa, etc. (Figure 13b). Correspondingly, the SPD group

takes less time for the wind–pressure or gradient wind balance relationship to adjust in the model. Moreover, the relatively high specific humidity in the boundary layer favors intensification of the TC by providing more moisture to the inner core. The height and strength of the warm core are closely linked to the height reached by the maximum of vertical velocity around the eyewall (Holland, 1997; Vigh & Schubert, 2009). An intense warm core in combination with a greater updraft and stronger convection around the eyewall results in greater latent heat conversion into the kinetic and potential energy of the storms (Ge et al., 2013; Wu et al., 2015). These may be several key factors in the intensification of the TC. The above processes lead to only a slight adjustment in the storm structure in the first 3 hr of forecasts, following which the average forecast of the TC intensity is roughly comparable to that for the control member.

Overall, the different temporal evolution of the TC intensity could be attributed to the variations in the initial conditions, such as the gradient wind balance relationship, the intensity of the warm core in the upper levels, the perturbations of moisture in the lower levels, and the secondary circulation, between the SPU and SPD groups. The collective impact of these differences is the primary cause of the SPD issue. Therefore, an effective way to address this issue is by improving initial conditions. In addition, due to the reset of vertical velocity and hydrometeors to zero upon initialization in the model, the SPU process in both groups could potentially take longer than 6 hr. To address this issue more effectively, it is necessary to develop new data assimilation algorithms and model initialization methods that can generate a plausible secondary circulation at the initial time.

Data Availability Statement

The ensemble experiments were conducted using the OSCER supercomputer at the University of Oklahoma. The boundary conditions for the outermost domain in the ensemble experiments can be downloaded from National Centers for Environmental Prediction (NCEP) (available at https://rda.ucar.edu/datasets/ds084.1/) [Dataset]. The best-track estimates for Hurricane Patricia (2015) can be downloaded from the National Centers for Environmental Information (available at https://www.ncei.noaa.gov/products/international-best-track-archive) (Knapp et al., 2018) [Dataset].

Acknowledgments
This research was jointly supported by the National Natural Science Foundation of China (Grants 42105059 and 42225501). This research was supported by the National Key Scientific and Technological Infrastructure project "Earth System Numerical Simulation Facility" (EarthLab). The first author was supported by the China Scholarship Council for a 1-year period of study at the University of Oklahoma. The second and third authors were supported by Grant NA16NWS4680028.

References

Bernardet, L., Tallapragada, V., Holt, C., Trahan, S., Biswas, M., Carson, L., et al. (2015). Transition of research to the operational hurricane WRF model: The role of the developmental testbed center. In *Paper presented at the sixth NOAA testbeds and proving grounds workshop*. NOAA. Retrieved from https://www.testbeds.noaa.gov/events/2015/workshop/presentations/wed-bernardet-hwrf.pdf

Chandrasekar, R., & Balaji, C. (2016). Impact of physics parameterization and 3DVAR data assimilation on prediction of tropical cyclones in the Bay of Bengal region. *Natural Hazards*, *80*(1), 223–247. https://doi.org/10.1007/s11069-015-1966-5

Chavas, D. R., Reed, K. A., & Knaff, J. A. (2017). Physical understanding of the tropical cyclone wind-pressure relationship. *Nature Communications*, *8*(1), 1360. https://doi.org/10.1038/s41467-017-01546-9

Chen, L., Duan, W. S., & Xu, H. (2015). A SVD-based ensemble projection algorithm for calculating the conditional nonlinear optimal perturbation. *Science China Earth Sciences*, *58*(3), 385–394. https://doi.org/10.1007/s11430-014-4991-4

Ek, M. B., Mitchell, K. E., Lin, Y., Rogers, E., Grummann, P., Koren, V., et al. (2003). Implementation of Noah land surface model advances in the National Centers for Environmental Prediction operational mesoscale Eta model. *Journal of Geophysical Research*, *108*(D22), 8851. https://doi.org/10.1029/2002JD003296

Emanuel, K., Weng, Y., Sippel, J. A., Braun, S. A., Munsell, E. B., Zhang, F., & Nystrom, R. G. (2018). Predictability and dynamics of Hurricane Joaquin (2015) explored through convection-permitting ensemble sensitivity experiments. *Journal of the Atmospheric Sciences*, *75*(2), 401–424. https://doi.org/10.1175/JAS-D-17-0137.1

Emanuel, K., & Zhang, F. Q. (2016). On the predictability and error sources of tropical cyclone intensity forecasts. *Journal of the Atmospheric Sciences*, *73*(9), 3739–3747. https://doi.org/10.1175/JAS-D-16-0100.1

Emanuel, K., & Zhang, F. Q. (2017). The role of inner-core moisture in tropical cyclone predictability and practical forecast skill. *Journal of the Atmospheric Sciences*, *74*(7), 2315–2324. https://doi.org/10.1175/JAS-D-17-0008.1

Feng, J., Qin, X., Wu, C., Zhang, P., Yang, L., Shen, X., et al. (2022). Improving typhoon predictions by assimilating the retrieval of atmospheric temperature profiles from the FengYun-4A's Geostationary Interferometric Infrared Sounder (GIIRS). *Atmospheric Research*, *280*, 106391. https://doi.org/10.1016/j.atmosres.2022.106391

Feng, J., & Wang, X. (2019). Impact of assimilating upper-level dropsonde observations collected during the TCI field campaign on the prediction of intensity and structure of Hurricane Patricia (2015). *Monthly Weather Review*, *147*(8), 3069–3089. https://doi.org/10.1175/MWR-D-18-0305.1

Feng, J., & Wang, X. (2021). Impact of increasing horizontal and vertical resolution during the HWRF hybrid EnVar data assimilation on the analysis and prediction of Hurricane Patricia (2015). *Monthly Weather Review*, *149*(2), 419–441. https://doi.org/10.1175/MWR-D-20-0144.1

Ge, X., Li, T., & Peng, M. (2013). Effects of vertical shears and midlevel dry air on tropical cyclone developments. *Journal of the Atmospheric Sciences*, *70*(12), 3859–3875. https://doi.org/10.1175/jas-d-13-066.1

Goldenberg, S. B., Gopalakrishnan, S. G., Tallapragada, V., Quirino, T., Marks, F., Trahan, S., et al. (2015). The 2012 triply nested, high-resolution operational version of the Hurricane Weather Research and Forecasting Model (HWRF): Track and intensity forecast verifications. *Weather and Forecasting*, *30*(3), 710–729. https://doi.org/10.1175/waf-d-14-00098.1

Gopalakrishnan, S. G., Upadhayay, S., Jung, Y., Marks, F., Tallapragada, V., Mehra, A., et al. (2018). 2017 HFIP R&D activities summary: Recent results and operational implementation. In *NOAA HFIP tech. Rep. HFIP2018-1* (p. 34) Retrieved from http://www.hfip.org/documents/HFIP_AnnualReport_FY2017.pdf

Guo, X., & Tan, Z. M. (2017). Tropical cyclone fullness: A new concept for interpreting storm intensity. *Geophysical Research Letters*, *44*(9), 4324–4331. https://doi.org/10.1002/2017GL073680

Han, J., & Pan, H.-L. (2006). Sensitivity of hurricane intensity forecast to convective momentum transport parameterization. *Monthly Weather Review*, *134*(2), 664–674. https://doi.org/10.1175/mwr3090.1

Heng, J., & Wang, Y. (2016). Nonlinear response of a tropical cyclone vortex to prescribed eyewall heating with and without surface friction in TCM4: Implications for tropical cyclone intensification. *Journal of the Atmospheric Sciences*, *73*(3), 1315–1333. https://doi.org/10.1175/jas-d-15-0164.1

Holland, G. J. (1997). The maximum potential intensity of tropical cyclones. *Journal of the Atmospheric Sciences*, *54*(21), 2519–2541. https://doi.org/10.1175/1520-0469(1997)054<2519:tmpiot>2.0.co;2

Hong, S.-Y., & Pan, H.-L. (1996). Nonlocal boundary layer vertical diffusion in a medium-range forecast model. *Monthly Weather Review*, *124*(10), 2322–2339. https://doi.org/10.1175/1520-0493(1996)124<2322:nblvdi>2.0.co;2

Johnson, A., Wang, X., Kong, F., & Xue, M. (2011). Hierarchical cluster analysis of a convection-allowing ensemble during the Hazardous Weather Testbed 2009 Spring Experiment. Part I: Development of the object-oriented cluster analysis method for precipitation fields. *Monthly Weather Review*, *139*(12), 3673–3693. https://doi.org/10.1175/mwr-d-11-00015.1

Kaplan, J., & DeMaria, M. (2003). Large-scale characteristics of rapidly intensifying tropical cyclones in the North Atlantic basin. *Weather and Forecasting*, *18*(6), 1093–1108. https://doi.org/10.1175/1520-0434(2003)018<1093:lcorit>2.0.co;2

Kimberlain, T. B., Blake, E. S., & Cangialosi, J. P. (2015). Hurricane Patricia (EP202015): National Hurricane Center tropical cyclone report (p. 32). Retrieved from https://www.nhc.noaa.gov/data/tcr/EP202015_Patricia.pdf

Knaff, J. A., & Zehr, R. M. (2007). Reexamination of tropical cyclone pressure—Wind relationships. *Weather and Forecasting*, *22*(1), 71–88. https://doi.org/10.1175/waf965.1

Knapp, K. R., Diamond, H. J., Kossin, J. P., Kruk, M. C., & Schreck, C. J. (2018). International best track archive for climate stewardship (IBTrACS) project, version 4 [indicate subset used] [Dataset]. NOAA National Centers for Environmental Information. https://www.ncei.noaa.gov/products/international-best-track-archive

Kwon, Y. C., Lord, S., Lapenta, B., Tallapragada, V., Liu, Q., & Zhang, Z. (2010). Sensitivity of air-sea exchange coefficients (Cd and Ch) on hurricane intensity. In *29th conference on Hurricanes and tropical meteorology*.

Lacis, A. A., & Hansen, J. (1974). A parameterization for the absorption of solar radiation in the earth's atmosphere. *Journal of the Atmospheric Sciences*, *31*(1), 118–133. https://doi.org/10.1175/1520-0469(1974)031<0118:apftao>2.0.co;2

Lang, S., Leutbecher, M., & Jones, S. (2012). Impact of perturbation methods in the ECMWF ensemble prediction system on tropical cyclone forecasts. *The Quarterly Journal of the Royal Meteorological Society*, *138*(669), 2030–2046. https://doi.org/10.1002/qj.1942

Li, X., & Pu, Z. (2008). Sensitivity of numerical simulation of early rapid intensification of Hurricane Emily (2005) to cloud microphysical and planetary boundary layer parameterizations. *Monthly Weather Review*, *136*(12), 4819–4838. https://doi.org/10.1175/2008mwr2366.1

Liu, Q., Lord, S., Surgi, N., Zhu, Y., Wobus, R., Toth, Z., & Marchok, T. (2006). Hurricane relocation in global ensemble forecast system. In *27th conference on Hurricanes and tropical meteorology, Monterey, CA* (p. 5.13). A. M. Society.

Liu, Q., Zhang, X., Tong, M., Zhang, Z., Liu, B., Wang, W., et al. (2020). Vortex initialization in the NCEP operational hurricane models. *Atmosphere*, *11*(9), 968. https://doi.org/10.3390/atmos11090968

Lu, X., & Wang, X. (2019). Improving hurricane analyses and predictions with TCI, IFEX field campaign observations, and CIMSS AMVs using the advanced hybrid data assimilation system for HWRF. Part I: What is missing to capture the rapid intensification of hurricane Patricia (2015) when HWRF is already initialized with a more realistic analysis? *Monthly Weather Review*, *147*(4), 1351–1373. https://doi.org/10.1175/mwr-d-18-0202.1

Lu, X., & Wang, X. (2021). Improving the four-dimensional incremental analysis update (4DIAU) with the HWRF 4DEnVar data assimilation system for rapidly evolving hurricane prediction. *Monthly Weather Review*, *149*, 4027–4043. https://doi.org/10.1175/mwr-d-21-0068.1

Lu, X., Wang, X., Li, Y., Tong, M., & Ma, X. (2017). GSI-Based ensemble-variational hybrid data assimilation for HWRF for hurricane initialization and prediction: Impact of various error covariances for airborne radar observation assimilation. *The Quarterly Journal of the Royal Meteorological Society*, *143*(702), 223–239. https://doi.org/10.1002/qj.2914

Lu, X., Wang, X., Tong, M., & Tallapragada, V. (2017). GSI-based, continuously cycled, dual-resolution hybrid ensemble–variational data assimilation system for HWRF: System description and experiments with Edouard (2014). *Monthly Weather Review*, *145*(12), 4877–4898. https://doi.org/10.1175/mwr-d-17-0068.1

Martinez, J., Bell, M. M., Rogers, R. F., & Doyle, J. D. (2019). Axisymmetric potential vorticity evolution of Hurricane Patricia (2015). *Journal of the Atmospheric Sciences*, *76*(7), 2043–2063. https://doi.org/10.1175/JAS-D-18-0373.1

Pu, Z., Li, X., & Sun, J. (2009). Impact of airborne Doppler radar data assimilation on the numerical simulation of intensity changes of Hurricane Dennis near a landfall. *Journal of the Atmospheric Sciences*, *66*(11), 3351–3365. https://doi.org/10.1175/2009jas3121.1

Pu, Z., Zhang, S., Tong, M., & Tallapragada, V. (2016). Influence of the self-consistent regional ensemble background error covariance on hurricane inner-core data assimilation with the GSI-based hybrid system for HWRF. *Journal of the Atmospheric Sciences*, *73*(12), 4911–4925. https://doi.org/10.1175/jas-d-16-0017.1

Qin, N. N., & Zhang, D. L. (2018). On the extraordinary intensification of hurricane Patricia (2015). Part I: Numerical experiments. *Weather and Forecasting*, *33*(5), 1205–1224. https://doi.org/10.1175/Waf-D-18-0045.1

Rogers, R. F., Aberson, S., Bell, M. M., Cecil, D. J., Doyle, J. D., Kimberlain, T. B., et al. (2017). Rewriting the tropical cyclone record books: The extraordinary intensification of Hurricane Patricia (2015). *Bulletin of the American Meteorological Society*, *98*(10), 2091–2112. https://doi.org/10.1175/Bams-D-16-0039.1

Schoenberg Ferrier, B. (1994). A double-moment multiple-phase four-class bulk ice scheme. Part I: Description. *Journal of the Atmospheric Sciences*, *51*(2), 249–280. https://doi.org/10.1175/1520-0469(1994)051<0249:admmpf>2.0.co;2

Schwarzkopf, M. D., & Fels, S. B. (1991). The simplified exchange method revisited: An accurate, rapid method for computation of infrared cooling rates and fluxes. *Journal of Geophysical Research*, *96*(D5), 9075–9096. https://doi.org/10.1029/89jd01598

Serafin, S., Strauss, L., & Dorninger, M. (2019). Ensemble reduction using cluster analysis. *Quarterly Journal of the Royal Meteorological Society*, *145*(719), 659–674. https://doi.org/10.1002/qj.3458

Shi, D., & Chen, G. (2021). Double warm-core structure and potential vorticity diagnosis during the rapid intensification of Supertyphoon Lekima (2019). *Journal of the Atmospheric Sciences*, *78*, 2471–2492. https://doi.org/10.1175/jas-d-20-0383.1

Smith, R. K., Montgomery, M. T., & Van Sang, N. (2009). Tropical cyclone spin-up revisited. *The Quarterly Journal of the Royal Meteorological Society*, *135*(642), 1321–1335. https://doi.org/10.1002/qj.428

Stern, D. P., & Nolan, D. S. (2012). On the height of the warm core in tropical cyclones. *Journal of the Atmospheric Sciences*, *69*(5), 1657–1680. https://doi.org/10.1175/jas-d-11-010.1

Stern, D. P., & Zhang, F. (2013). How does the eye warm? Part I: A potential temperature budget analysis of an idealized tropical cyclone. *Journal of the Atmospheric Sciences*, *70*(1), 73–90. https://doi.org/10.1175/jas-d-11-0329.1

Sun, X., Xie, L., Shah, S. U., & Shen, X. (2021). A machine learning based ensemble forecasting optimization algorithm for preseason prediction of Atlantic hurricane activity. *Atmosphere*, *12*(4), 522. https://doi.org/10.3390/atmos12040522

Tallapragada, V., Bernardet, L., Biswas, M. K., Gopalakrishnan, S., Kwon, Y., Liu, Q., et al. (2014). *Hurricane weather research and forecasting (HWRF) model: 2014 scientific documentation* (p. 105). NCAR Development Testbed Center Report. Retrieved from http://www.dtcenter.org/HurrWRF/users/docs/scientific_documents/HWRFv3.6a_ScientificDoc.pdf

Tao, D., Van Leeuwen, P. J., Bell, M., & Ying, Y. (2022). Dynamics and predictability of tropical cyclone rapid intensification in ensemble simulations of Hurricane Patricia (2015). *Journal of Geophysical Research: Atmospheres*, *127*(8), e2021JD036079. https://doi.org/10.1029/2021jd036079

Tao, D., & Zhang, F. (2014). Effect of environmental shear, sea-surface temperature, and ambient moisture on the formation and predictability of tropical cyclones: An ensemble-mean perspective. *Journal of Advances in Modeling Earth Systems*, *6*(2), 384–404. https://doi.org/10.1002/2014ms000314

Tao, D., & Zhang, F. (2019). Evolution of dynamic and thermodynamic structures before and during rapid intensification of tropical cyclones: Sensitivity to vertical wind shear. *Monthly Weather Review*, *147*(4), 1171–1191. https://doi.org/10.1175/mwr-d-18-0173.1

Thu, T. V., & Krishnamurti, T. (1992). Vortex initialization for typhoon track prediction. *Meteorology and Atmospheric Physics*, *47*(2–4), 117–126. https://doi.org/10.1007/bf01025612

Van Sang, N., Smith, R. K., & Montgomery, M. T. (2008). Tropical-cyclone intensification and predictability in three dimensions. *The Quarterly Journal of the Royal Meteorological Society*, *134*(632), 563–582. https://doi.org/10.1002/qj.235

Vigh, J. L., & Schubert, W. H. (2009). Rapid development of the tropical cyclone warm core. *Journal of the Atmospheric Sciences*, *66*(11), 3335–3350. https://doi.org/10.1175/2009jas3092.1

Vukicevic, T., Aksoy, A., Reasor, P., Aberson, S. D., Sellwood, K. J., & Marks, F. (2013). Joint impact of forecast tendency and state error biases in ensemble Kalman filter data assimilation of inner-core tropical cyclone observations. *Monthly Weather Review*, *141*(9), 2992–3006. https://doi.org/10.1175/mwr-d-12-00211.1

Weidle, F., Wang, Y., Tian, W., & Wang, T. (2013). Validation of strategies using clustering analysis of ECMWF EPS for initial perturbations in a limited area model ensemble prediction system. *Atmosphere-Ocean*, *51*(3), 284–295. https://doi.org/10.1080/07055900.2013.802217

Wu, L., Su, H., Fovell, R. G., Dunkerton, T. J., Wang, Z., & Kahn, B. H. (2015). Impact of environmental moisture on tropical cyclone intensification. *Atmospheric Chemistry and Physics*, *15*(24), 14041–14053. https://doi.org/10.5194/acp-15-14041-2015

Yanai, M. (1964). Formation of tropical cyclones. *Reviews of Geophysics*, *2*, 367–414. https://doi.org/10.1029/rg002i002p00367

Yussouf, N., Stensrud, D. J., & Lakshmivarahan, S. (2004). Cluster analysis of multimodel ensemble data over New England. *Monthly Weather Review*, *132*(10), 2452–2462. https://doi.org/10.1175/1520-0493(2004)132<2452:caomed>2.0.co;2

Zhang, B., Lindzen, R. S., Tallapragada, V., Weng, F., Liu, Q., Sippel, J. A., et al. (2016). Increasing vertical resolution in US models to improve track forecasts of Hurricane Joaquin with HWRF as an example. *Proceedings of the National Academy of Sciences*, *113*(42), 11765–11769. https://doi.org/10.1073/pnas.1613800113

Zhang, D. L., & Chen, H. (2012). Importance of the upper-level warm core in the rapid intensification of a tropical cyclone. *Geophysical Research Letters*, *39*(2), L02806. https://doi.org/10.1029/2011GL050578

Zhang, F., Weng, Y., Gamache, J. F., & Marks, F. D. (2011). Performance of convection–permitting hurricane initialization and prediction during 2008–2010 with ensemble data assimilation of inner–core airborne Doppler radar observations. *Geophysical Research Letters*, *38*(15), L15810. https://doi.org/10.1029/2011gl048469

Zhang, F. Q., & Sippel, J. A. (2009). Effects of moist convection on hurricane predictability. *Journal of the Atmospheric Sciences*, *66*(7), 1944–1961. https://doi.org/10.1175/2009jas2824.1

Zhang, Z., Tong, M., Sippel, J. A., Mehra, A., Zhang, B., Wu, K., et al. (2020). The impact of stochastic physics-based hybrid GSI/EnKF data assimilation on hurricane forecasts using EMC operational hurricane modeling system. *Atmosphere*, *11*(8), 801. https://doi.org/10.3390/atmos11080801

Zheng, Y., Wu, L., Zhao, H., Zhou, X., & Liu, Q. (2020). Simulation of extreme updrafts in the tropical cyclone eyewall. *Advances in Atmospheric Sciences*, *37*(7), 781–792. https://doi.org/10.1007/s00376-020-9197-4

Zhong, Q. J., Wang, X. G., Ding, R. Q., Lu, X., Huang, Y., Duan, W., & Liu, L. (2022). Impact of the low wavenumber structure in the initial vortex wind analyses on the prediction of the intensification of Hurricane Patricia (2015). *Journal of Geophysical Research: Atmospheres*, *128*(2), e2022JD037082. https://doi.org/10.1029/2022JD037082

Zhou, C., Shao, H., & Bernardet, L. (2015). Applications of the GSI-hybrid data assimilation for high-resolution tropical storm forecasts: Tackling the intensity spin-down issue in 2014 HWRF. In *16th WRF users workshop, Boulder, CO*.